Technical Note

CEL

TN no. N-1501

title: A SELF-CONTAINED EXPERIMENTAL DIVER HEATER

author: S. A. Black and S. S. Sergev

date: September 1977

sponsor: NAVAL SEA SYSTEMS COMMAND

program nos: 43-015

CIVIL ENGINEERING LABORATORY
NAVAL CONSTRUCTION BATTALION CENTER
Port Hueneme, California 93043

DISCLAIMER NOTICE

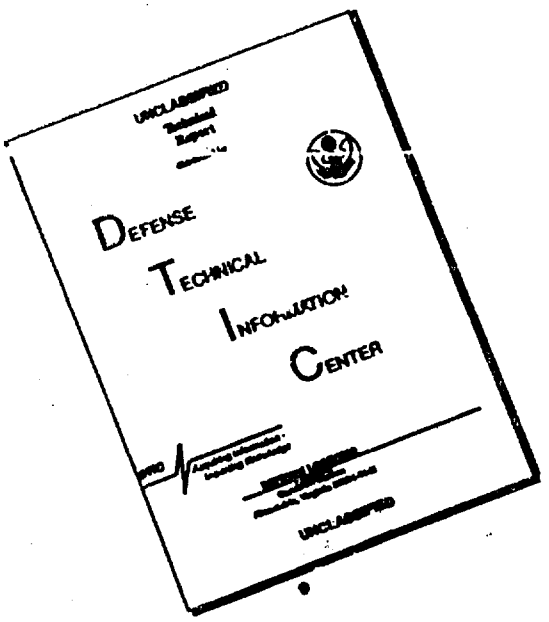

THIS DOCUMENT IS BEST QUALITY AVAILABLE. THE COPY FURNISHED TO DTIC CONTAINED A SIGNIFICANT NUMBER OF PAGES WHICH DO NOT REPRODUCE LEGIBLY.

Unclassified

SECURITY CLASSIFICATION OF THIS PAGE (When Data Entered)

REPORT DOCUMENTATION PAGE

READ INSTRUCTIONS BEFORE COMPLETING FORM

1. REPORT NUMBER: TN-1501	2. GOVT ACCESSION NO: DN244151
3. RECIPIENT'S CATALOG NUMBER	
4. TITLE (and Subtitle): A SELF-CONTAINED EXPERIMENTAL DIVER HEATER	5. TYPE OF REPORT & PERIOD COVERED: Not final; Sep 1973–Feb 1977
	6. PERFORMING ORG. REPORT NUMBER
7. AUTHOR(s): S. A. Black and S. S. Sergev	8. CONTRACT OR GRANT NUMBER(s)
9. PERFORMING ORGANIZATION NAME AND ADDRESS: CIVIL ENGINEERING LABORATORY, Naval Construction Battalion Center, Port Hueneme, California 93043	10. PROGRAM ELEMENT, PROJECT, TASK AREA & WORK UNIT NUMBERS: 63713N; S4619; 1620871; 43-015
11. CONTROLLING OFFICE NAME AND ADDRESS: Naval Sea Systems Command, Washington, D.C. 20362	12. REPORT DATE: September 1977
	13. NUMBER OF PAGES: 76
14. MONITORING AGENCY NAME & ADDRESS (if different from Controlling Office)	15. SECURITY CLASS (of this report): Unclassified
	15a. DECLASSIFICATION DOWNGRADING SCHEDULE

16. DISTRIBUTION STATEMENT (of this Report)

Approved for public release; distribution unlimited.

17. DISTRIBUTION STATEMENT (of the abstract entered in Block 20, if different from Report)

18. SUPPLEMENTARY NOTES

19. KEY WORDS (Continue on reverse side if necessary and identify by block number)

Diver-heating, electrochemical heat source, magnesium-seawater reaction, powdered metal electrochemical cell, human factors.

20. ABSTRACT (Continue on reverse side if necessary and identify by block number)

Free-swimming divers working in cold water for extended periods of time require a self-contained, active heat source to maintain their physiological thermal equilibrium. Previously, the accelerated reaction of magnesium with seawater was shown to be a suitable heat source for diving applications. The magnesium heat cell was configured as a short-circuited battery with alternate electrodes of magnesium and steel spaced closely together; the unit is activated by immersion in a seawater electrolyte. An

continued

DD FORM 1 JAN 73 1473 EDITION OF 1 NOV 65 IS OBSOLETE

Unclassified

SECURITY CLASSIFICATION OF THIS PAGE (When Data Entered)

391 111

20. Continued

experimental heater was fabricated that incorporated known improvements in the cell. The self-contained unit provided 1,000 watts for up to 8 hours. A human factors study was made that identifies heater configurations for closed-circuit scuba divers.

Library Card

Civil Engineering Laboratory
A SELF-CONTAINED EXPERIMENTAL DIVER HEATER,
by S. A. Black and S. S. Sergev
TN-1501 76 pp illus September 1977 Unclassified

1 Diver-heater 2. Electrochemical heat source I. 43-015

Free-swimming divers working in cold water for extended periods of time require a self-contained, active heat source to maintain their physiological thermal equilibrium. Previously, the accelerated reaction of magnesium with seawater was shown to be a suitable heat source for diving applications. The magnesium heat cell was configured as a short-circuited battery with alternate electrodes of magnesium and steel spaced closely together; the unit is activated by immersion in a seawater electrolyte. An experimental heater was fabricated that incorporated known improvements in the cell. The self-contained unit provided 1,000 watts for up to 8 hours. A human factors study was made that identifies heater configurations for closed-circuit scuba divers.

CONTENTS

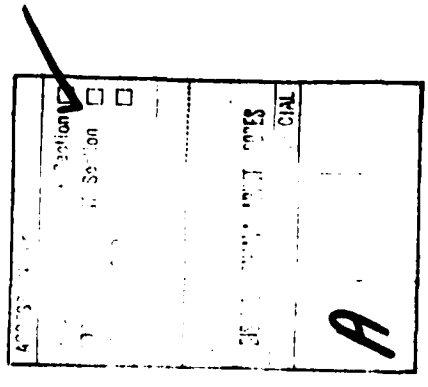

INTRODUCTION

Under the sponsorship of the Naval Sea Systems Command, the Civil Engineering Laboratory (CEL) has been engaged in the development of an experimental diver heater. The project objective is to develop a compact, portable, self-contained energy source capable of supplying heated water to a closed-loop circulation garment worn by the diver. Circulation garments and associated thermal protection gear are under development at the Naval Coastal Systems Laboratory (NCSL), Panama City, Florida. Basic requirements for the heater include operation in 28°F (-2°C) seawater at depths of 1,000 feet (305 m) for up to 8 hours without replenishment. Experimental models of 8- and 16-kWh (28.8- and 57.6-MJ) capacity were developed and laboratory tested. In addition the 8-kWh (28.8-MJ) unit was successfully diver-tested, proving the feasibility of the magnesium/seawater heat source.

BACKGROUND

Divers exposed to cold water for extended periods of time require thermal protection equipment to maintain acceptable physiological conditions and operational effectiveness. The overall heating problem is that of maintaining the diver's normal thermal balance. The amount of heat required varies with environmental factors, such as water depth, breathing gas type, water temperature, and duration of exposure, and with individual factors, such as physical condition, metabolic rate, and activity level. Thermal balance can be expressed by the simplified equation:

Heat Replacement = Respiratory heat loss + diving suit loss
- metabolic heat generated

Respiratory losses are due to involuntary heating of inspired gas to body temperature prior to expiration. The amount can be up to about 500 watts [1] depending upon the specific heat, density, volume, and temperature of the inspired gas. Diving suit losses vary with depth, type of suit, suit material, and water temperature. The values range from 3,000 watts for the standard 3/8-inch (9.5-mm) thick neoprene wet suit [19 ft^2 (1.75m^2) surface area] at 1,000-foot (305-m) depth with a skin-to-seawater temperature difference of 50°F (28°C), to 1,000 watts for a dry suit

filled with helium under the same conditions [2].* The metabolic heat generated varies with individual activity level and physical condition and ranges from near zero for inactive divers to as much as 500 watts for sustained heavy work periods. To insure adequate heat would be available to maintain thermal balance under extreme conditions, an initial program goal of 2,000 watts was selected as the heater output.

Heating is required both for tethered and self-contained divers. The present method for heating the tethered diver is to supply hot water via an umbilical hose from the support platform (surface ship, PTC, etc). The hot water is flushed over the diver's body under his diving suit and then exhausted directly to the surrounding environment. In this case, the physical size and weight of the heat source is not critical, since it is not carried by the diver. However, because of both the high heat losses in hoses and the open-circuit design, the system is grossly inefficient. In addition, the hot water umbilical greatly restricts the diver's mobility.

For the free-swimming diver, thermal protection is not easily provided. Since the heat source must be carried on his person, it must be lightweight and compact and not impair his mobility. In addition it must be simple, safe, and reliable.

In the past, several methods of providing heat for free-swimming divers have been investigated [3-11]. The resulting systems have exhibited several disadvantages: batteries are heavy, bulky, expensive, and short-lived; nuclear sources can be used by the diver only for short durations because of radiation exposure, and the radiation shielding and thermal safety devices make the nuclear heater bulky and complicated; and most thermochemical heat sources employ exotic reactants and involve high operating temperatures and complicated control systems.

A compact, lightweight, high-energy density, easily controlled, reliable, safe heat source that can be integrated with closed-circuit hot water suits is vitally needed. To this end, CEL has been investigating the development of a heater that utilizes the reaction of a magnesium alloy with seawater to produce heat.

HEAT SOURCE DEVELOPMENT

Background

The oxidation reaction of magnesium was chosen for the heat source, because it is simple, reliable, compact, and inexpensive, and has a comparatively high-energy density. A comparison of the CEL-developed

---

*Ongoing research being conducted at NCSL in thermal protection suits is expected to produce significant improvements in this area.

heat source with other candidates is shown in Table 1.

Magnesium reacts with seawater according to Equation 1:

$$Mg + 2H_2O \rightarrow Mg(OH)_2 + H_2\ (gas) + \Delta h \qquad (1)$$

where Δh is the heat of formation of the reaction.

The theoretical energy density of this reaction is 1,885 W-hr/lb of magnesium (14.9 MJ/kg). The reaction ordinarily proceeds slowly in seawater, and heat is not released at a usable rate. But, by electrically connecting the magnesium to a cathodic material, such as iron (forming a galvanic couple), the reaction proceeds much more rapidly and liberates heat at a usable rate. Similar systems have been developed as seawater batteries.

The CEL heater uses the same basic principle as the seawater battery, but the battery's external load is replaced by a short circuit to maximize the reaction rate. A simplified schematic model of the reaction process is shown in Figure 1. Major steps of the process are:

1. Current flows from anode to cathode via the short circuit because of the potential difference.

2. Water is reduced at the cathode.

3. Magnesium ions are formed at the anode.

4. Hydroxide and magnesium ions migrate to a point where they combine to form magnesium hydroxide.

Chemical energy is converted into thermal energy by means of a highly efficient electrochemical reaction. The energy given off by this reaction heats the surrounding electrolyte. A more detailed discussion of the reaction process is contained in Reference 12.

The basic heat-producing element of the electrochemical reaction is the dual-plate cell shown in Figure 2. The spacer washer provides both an electrode gap and a short circuit current path. The electrode gap provides for free passage of the electrolyte and removal of the reaction products [H_2 and $Mg(OH)_2$]. As the magnesium is reacted, the anode becomes thinner and the electrode gap increases.

It is important for the spacer washer to provide a very low resistance path (less than 10^{-3} ohms) for current flow. With a high resistance path, part of the energy goes into inefficient electrical Joule heating, and the reaction rate* is reduced to unusable values in terms of diver heating.

*Reaction rate is defined as power output per unit-surface-area of anode.

Experimental Arrangement

Early experimental work showed that the reaction rate of the dual-plate cell is a function of several interdependent parameters. The most important of these parameters are electrolyte temperature, electrode gap, and electrolyte condition. In an attempt to isolate and understand the effects of these and other parameters, a number of laboratory experiments were conducted.

Three different configurations were utilized in the laboratory experimentation. Quantitative data on reaction parameters were obtained using an insulated Dewar flask (Figure 3) that was accurately calibrated for heat loss. The test cells consisted of three magnesium and four iron plates of up to 72 $in.^2$ (465 cm^2) of anode surface area. A pump was provided to test the effects of electrolyte circulation on cell performance. The temperature rise of the electrolyte was recorded on a multipoint recorder.

Uninsulated glass beakers were used for tests in which only qualitative results were needed. The results were obtained by visually inspecting the anodes and by monitoring temperature differences between several cells running simultaneously in different beakers.

A third apparatus was used for testing cells of up to 1,000 $in.^2$ (0.645 m^2) of anode surface area (Figure 4). The cell and electrolyte were contained in an insulated acrylic case with a removable top. Thermocouples were provided for monitoring the temperature of the circulating electrolyte. A second fluid was circulated through a copper tube heat exchanger immersed in the cell electrolyte and through external cooling coils. In this manner the electrolyte could be maintained at a constant temperature. Temperature change and flow rate of the second fluid were used to determine power output. An additional method was provided for adding controlled amounts of fresh seawater the reaction chamber.

Dual-Plate Cell

The dual-plate cell consists of separate anode and cathode plates arranged as shown in Figure 5. Over 70 tests were run in the Dewar to determine the effect of the various parameters on cell performance. The major objectives were to determine the effects of electrode gap and electrolyte temperature on reaction rate and reaction efficiency.* The initial gap, which was set prior to the start of each test, ranged from 0.060 (0.15 cm) to 0.200 (0.5 cm) inch. At each spacing the temperature was allowed to rise $60^{\circ}F$ ($30^{\circ}C$). Starting temperatures varied from $30^{\circ}F$ ($-1^{\circ}C$) to $150^{\circ}F$ ($65^{\circ}C$) in $20^{\circ}F$ ($11^{\circ}C$) increments.

---

*Reaction efficiency: ratio of actual energy output to theoretical energy output.

The relationship between energy density (W-hr per pound of magnesium), temperature, and spacing is shown in Figure 6. Energy density is shown to be a strong function of temperture and a relatively weak function of plate spacing. Based on theory it was expected that energy density would increase with temperature. The experimental results, however, show a marked decrease at the higher temperatures. This effect at the high reaction rates is caused by unused magnesium sloughing from the plates. The sloughed magnesium can be seen as small, dark-colored particles circulating in the electrolyte. Figure 6 shows that an energy-efficient reaction rate occurs between 100°F and 150°F (38° and 66°C).

The effects of plate spacing and temperature on power density are shown in Figure 7. As expected, the reaction rate proceeds more rapidly at higher temperatures and closer spacings.

The electrolyte condition is described in terms of pH, salinity, and density. Theory predicts that the reaction rate is reduced by high pH, low salinity, and increased density (resulting from reaction products mixing with the seawater electrolyte). To some extent the electrolyte density and pH can be controlled. But, in general, the heater must be designed to accommodate the natural variability of the seawater enviroment.

The pH, salinity, and conductivity of the electrolyte were measured to determine quantitatively how these parameters affected cell performance. For these parametric tests, the pH changed relatively little, because the comparatively large volume of seawater diluted the reaction product concentration. In addition, since seawater is a very good buffer, large quantities of $Mg(OH)_2$ would be required to make significant pH changes. Generally speaking, the reaction rate was affected as expected. Table 2 summarizes the effects of these and other parameters on cell performance, but no quantitative trends were identified.

Reaction Rate Decay Characteristics. To verify the results of the parametric tests, a series of large-scale tests were run in the acrylic vessel. In these tests fresh electrolyte was added at a controlled rate (125 ml/min), and an equal volume of slurry [$Mg(OH)_2$ and water] was removed to maintain constant electrolyte pH and density. The results of a typical test are shown in Figure 8. The broken line shows the estimated decay in cell power as predicted from parametric tests and based on anode consumption and increasing electrode gap. These results verified the fact that reaction is strongly dependent on electrode gap.

The power output during the first hour was significantly higher than predicted. The increase is attributed to several factors: clean anodes and low electolyte pH and density. Initially, the anodes are clean and free from reaction products, but during the first hour, magnesium hydroxide accumulates on the anode surface. These deposits inhibit the reaction process at the anode and subsequently reduce the overall reaction rate. Also, fresh seawater, which is a very good buffer, has a

relatively low pH and is very fluid. However, as the reaction products accumulate, both the pH and density increase so that, by the end of the first hour, stabilized values have been established based on the slurry removal and electrolyte addition rate. Although the full effect of these parameters is not understood, it is known that a high pH and a thick slurry can block the anodic reaction thereby reducing the reaction rate.

These factors appear to account for a large portion of the initially high reaction rate, but they are augmented by the anode edge reaction. New plates have a substantial edge area that is not normally used in power calculations. However, this area apparently contributes to the initial reaction rate (dotted line). As the reaction proceeds, the edge area diminishes; in fact, the plate dimensions are reduced as shown in Figure 9.

As would be expected, the high initial reaction rate from the above factors results in rapid magnesium comsumption during the first hour. The rate of consumption decays rapidly until an electrolyte equilibrium condition is attained. At this point (1-1/2 to 2 hours into the test) the consumption rate is governed primarily by electrode gap, which is evidenced by the similar slopes of the dashed and solid lines during the remaining test hours (Figure 8). Because of the high initial reaction and early electrode gap increases, the reaction rate is lower than predicted from the parametric tests during the later hours of the test.

In accordance with the decaying power curve, a cell that delivers the desired power at the end of its operating period, delivers excess power initially. A number of tests were conducted to determine if the high initial and resultant low final rates could be better balanced to provide a flatter power curve; these tests are summarized in Table 3. The most effective modification was to alter the anode dimensions to reduce or eliminate the edge effect. This was accomplished by fabricating anodes of slightly larger dimensions than the cathode. Thus, the edge was located far enough away from the cathode to significantly reduce the edge effect. The modification was used on all subsequent dual-plate cell construction.

Other Parameters Affecting Reaction Rate. Variations in the cathode thickness and surface condition and in the electrolyte salinity affect the reaction rate. Thick cathodes have the lowest electrical resistance and produce the highest reaction rates (Figure 10). However, cathodes thicker than 0.060 inch (0.15 cm) do not noticeably improve cell performance. On the other hand, thin cathodes [0.001 in. (0.003 cm)] are desirable because they minimize weight, but they also warp, and, consequently, the electrode gap cannot be reliably maintained. A cathode thickness of 0.010 inch (0.03 cm) was selected as a compromise between minimum weight, reasonable structural strength, and power output.

It was discovered that the output of a cell with 0.010-inch thick cathodes could be increased by as much as 30% by sandblasting the cathode surface (Figure 11). The rough surface greatly increases the number of

sites available for hydrogen gas bubble nucleation. Other techniques for increasing the cathode surface area, such as scratching or sanding, produce similar, but less dramatic, effects.

Electrolyte salinity has a pronounced effect on the reaction rate. Figure 12 shows seawater (34 o/oo salinity) as a standard; however, salt-saturated seawater will produce a much higher reaction rate. This high rate will continue for only a short time (about 1 hour), because the reaction product, a jelly-like substance, will increase the electrolyte density and thereby reduce the reaction rate to an unusable level. Very few ions are present in an extremely low salinity electrolyte; therefore, the reaction rate of the cell will be negligible in terms of heat production. In general, the salinity and buffering quality of seawater combine to create the highest long-term reaction rate possible.

The thickness and surface condition of the cathode can easily be controlled to provide the desired power output. In general, the cell is subject to operation within the normal local salinity range. However, where required, rapid heat-up can be achieved by ''spiking'' the initial charge of seawater with salt. Normal electrolyte/seawater exchange will flush the jelly-like products from the cell chamber, reduce the salinity, and return the cell to the normal power level.

Reaction Control. The development of a reliable and simple control system for maintaining a constant power output was explored to reduce the size and weight of the cell to less than that of the fixed-plate cell. Table 4 summarizes the results of these investigations. The most promising method appears to be of the inert cone spacer (Figure 13), which uses the reaction itself to control spacing. As of now, a simplified method for assembling these cells and also providing the short circuit has not been developed. There are two major problems in each of the control techniques. First, cell construction becomes too complicated, and, second, the weight and volume of a cell plus control system exceed those of a cell designed to provide the same delivered final power without control.

A variety of other tests were performed in attempts to control or modify the reaction rate. These tests are summarized in Table 4. None of the test results showed improvements significant enough to cause modification of the basic dual-plate cell configuration.

Bi-Polar Electrode

One of the disadvantages of the dual-plate cell is holes start to form in the anode during the last hour of the reaction. The holes decrease the current-carrying cross section of the anode and reduce the active anode area. The result is reduced cell power. To minimize these effects in the dual-plate cell the anodes must be slightly thicker than actually needed. This insures enough active surface area will remain to provide the required power for the desired duration.

Another possible technique for avoiding this problem is to electroplate the cathodic material to one side of the anode. Thus, cell construction would be simplified by eliminating the need for a separate iron cathode. Also, cathodic and anodic currents would be shared. With this technique, as the anode thickness decreases, a constant thickness cathode remains to conduct a portion of the anodic current. An additional benefit is that the anode provides some structural strength to the cathode so that thinner cathodes could be used.

A 1,000-watt version of this cell was constructed and tested. The electroplating consisted of iron deposited onto a copper substrate that was plated onto one side of the magnesium. During the plating process, higher than normal plating currents were used to achieve the greatest possible cathode surface area (similar to sandblasted iron).

The cell produced approximately 20% more power than a comparable-area dual-plate cell (see Figure 11). This increase was probably due to (1) the measures taken to increase the surface area and (2) the low resistance electrical current path provided by the copper substrate.

To better understand the bi-polar electrode reaction, a single bi-polar electrode was placed in seawater. There was very little self-reaction, and it ocurred only near the edges of the electrode. This self-reaction rate was low because the current paths through the electrolyte were too long except at the edge; there the anode-cathode separation was only about 1/16 inch (0.16 cm) (approximately the electrode thickness).

Powdered Metal Cell

A preliminary investigation of magnesium and iron powder mixtures as possible heat sources is described in Reference 12. The tests included loose mixtures of size-graded magnesium and iron particles as well as mixtures of particles that had been mechanically bonded together by ball-milling* to produce microgalvanic cells. The results show that ball-milled mixtures produce the highest reaction rates and that the reaction is strongly influenced by particle size (area exposed to the electrolyte).

Further tests were conducted to develop a heat source with a greater specific output (W-hr/lb of cell) than the dual-plate cell [approximately 800 W-hr/lb of cell (6.3 MJ/kg)]. A means of controlling the heat output was also sought.

Small-scale tests were run to determine the best cathodic material for sustaining the reaction and the minimum percentage necessary to produce heat at a usable rate. The test results were compared by the rate of hydrogen evolution (directly related to power output) from five

*Ball-milling produces intimate contact between the particles.

gram samples of the candidate mixtures (Table 5). Mixtures of 10% by weight of copper or iron with magnesium gave the best combination of rate and efficiency at reasonable cost. Although the reaction rates of the magnesium-copper couple were higher, the magnesium-iron reacted at a more consistent rate over an extended period. As a result, the magnesium-iron couple was selected for larger scale tests.

The previous investigations addressed the power output control question by adding small amounts of seawater to the dry powder mixtures. When sufficient amounts of seawater were added to wet the entire powder volume, maximum power output was achieved; however, further additions of seawater had no appreciable effect. For the large-scale tests, control was attempted by metering the powder mixture into a chamber filled with seawater. The feasibility of controlling the reaction in this manner was proved; however, difficulty was encountered in adding the dry powder to the electrolyte.

To facilitate the addition of the reactants to the electrolyte, an effort was made to develop an inert slurry with the powder. A mixture of 50% morpheline and 50% powder formed a fairly stable slurry for pumping. However, the powder tended to settle out of the mixture, and the slurry was not completely inert; therefore, some reaction occurred within the slurry. A second slurry was prepared that resembled toothpaste in consistency. This gel was completely stable and did not react with the powder. Its composition was:

Constituent	Proportion (by weight)
Magnesium-iron powder	447.0
Carbowax® MPEG	394.0
Armeen® Z	<19.7
Cab-O-Sil®	3.0
Diethylenetriamine (DETA)	1.0

The slurry was added to the reaction chamber with a caulking gun. The large-scale tests showed that the slurry could be easily added to the seawater, but that continued stirring was necessary to keep the reaction at a constant rate. The slurrying agents were found to have no detrimental effect on the reaction. A specific output of approximately 500 W-hr/lb of reactant (3.95 MJ/kg) was achieved with the powdered metal reaction. With further development the specific output might be competitive with the dual-plate-type cell.

The most important result of the powdered metal tests is that an inert slurry has been developed. In slurry form, the powdered reactants can be supplied on a demand basis. By varying the slurry addition rate to a reaction chamber, power can be controlled.

Alloy Powder Tests

Although the powdered metal tests proved successful, the specific output was not as high as had been anticipated by having the anodic and cathodic materials in such close contact. Evidently, surface oxides on the metal (present during ball milling) acted as high resistance electrical barriers to the current flow.

To verify this theory, a magnesium-iron alloy was conceived in which intimate physical and electrical contact could be established between anode and cathode. Through conventional alloying only a very small percentage of iron (<<1% by weight) can be dissolved. This is much less than the 10% that proved optimum for the previous powdered metal tests. A process of mechanically alloying otherwise immiscible metals [13,14] has been established. In this process, magnesium and iron powders are milled in a high energy ball mill. The powder particles are cold-welded together as the balls in the mill collide. Repeated collisions cause particle fracturing and rewelding, and, eventually, a uniform alloy powder is formed.

Alloy samples were prepared and tested. Powder particle sizes were in two ranges: ''as-produced'' (larger than 100 mesh) and ''selected'' (smaller than 100 mesh). The initial tests showed that the as-produced samples reacted more effectively. An alloy particle would generate a gas bubble, rise to the water surface, release the bubble, and sink. On the other hand, the selected (finer) powder would not release its gas bubble. This resulted in a foam surface that actually lifted the powder particles out of the seawater and prevented them from reacting to completion. Thus, the remaining tests were conducted with the ''as-produced'' particle size.

Figure 14 shows the relationship of milling time to reaction efficiency. A maximum reaction efficiency of approximately 90% is approached asymptotically as shown in Figure 14a. Figure 14b shows the 30-minute milled alloy achieves almost this 90% completion in 1 minute. For additional tests the 30-minute milling time was used as the standard. (The rapid reaction completion time is desirable for using the alloy as a fuel.)

Initial alloy compositions were held constant at 5 atomic percent to show the effects of particle size and milling time. Another group of alloys of various iron percentages was tested to develop a family of curves that relate reaction efficiency and power output to alloy composition. These data are shown in Figures 15 and 16. The zero-percent ball-milled magnesium powder was tried to see if sufficient strain energy was stored in the particles to cause stress corrosion. As can be seen in Figure 15, some small amount of iron is required to produce a usable reaction. Alloys of several alternate cathodic materials were tested to see what reactions they would produce. These results are shown in

Figures 17 and 18. Nickel produced the only reaction that was competitive with iron. For other applications the data presented may aid in selecting an initial trial alloy composition.

Mechanically alloyed magnesium powders are well suited for a heater designed to deliver variable or constant power. At a reaction temperature of 140°F (60°C), approximately 0.01 pound (5 grams) of alloy (10% iron by weight) will produce 1,000 watts for 1 minute and will be 90% reacted. A possible configuration for a powder alloy heater is shown in Figure 19; its control circuitry is shown in Figure 20. The rapid and efficient reaction characteristics allow the powder to be fed continuously into the reaction tube with the assurance that only a small fraction of the available energy will be ejected from the tube as unreacted powder.

An estimate of energy density is 800 to 900 W-hr/lb of slurry (6.3 to 7.1 MJ/kg) compared with 500 W-hr/lb of slurry (3.95 MJ/kg) for the previous powdered metal tests. Thus, a highly efficient, variable power heater is conceivable using powdered magnesium alloy as an energy source.

Summary of Experimental Investigation

The experimental work demonstrated that the dual-plate cell could provide adequate power for the worst case (2,000-watt) diver application. The cell reaction rate was found to be a function of both electrode gap and electrolyte temperature. Other factors, such as electrolyte condition and circulation, affect cell operation to a much lesser degree. The most important factor that controls the overall cell effectiveness/performance is the power decay resulting from anode depletion (increasing electrode gap). Attempts to provide direct control to minimize this effect showed that inert cone spacers would be the best approach. A simple means for implementing the cone spacers while providing adequate anode/cathode flexible current paths is yet to be devised.

The bi-polar electrode cell offers simpler and more efficient construction than the dual-plate cell, but present anticipated cost of cell fabrication is excessive.

The powdered metal cell offers the advantage of controllable power output and, consequently, more efficient use of the magnesium. In the past, the disadvantage has been that the specific output was lower than the dual-plate cell. The magnesium-iron alloy (MagIron) powder appears to have a specific output competitive with the dual-plate cell because of a much lower electrical resistance. Further improvements in slurrying may increase the proportion of active to inert ingredients, thus increasing specific output. In such a case, the powdered alloy may prove to be superior to the dual-plate cell.

The characteristics of the three cell types are summarized in Table 6.

EXPERIMENTAL HEATER DEVELOPMENT

To demonstrate the feasibility of using the magnesium-iron couple as a self-contained heat source, two experimental heater models were developed. A 16-kW-hr model (Figure 21) was designed to provide 2,000 watts for 8 hours. The second unit, an 8-kW-hr model (Figure 22), was designed to provide 1,000 watts also for 8 hours. The discussion below refers in detail only to the 8-kW-hr heater, since it was developed last and incorporates improvements over the 16-kW-hr heater. However, important differences between them are discussed.

Operation

The magnesium-iron dual-plate cell is contained in the insulated case shown schematically in Figure 23. The heater is activated by flooding the case with seawater. Heat, hydrogen gas, and magnesium hydroxide are produced by the reaction. A heat exchanger immersed in the electrolyte transfers the generated heat to a second fluid that is circulated to the diver. Hydrogen gas is continuously vented through a valve that maintains a small overpressure within the case. This pressure drives a small amount of the slurry out through an economizer heat exchanger. Fresh seawater is pumped counterflow through the economizer to recover the heat from expelled hot slurry. The slurry and seawater exchange maintains the electrolyte pH and density relatively constant.

Heater Case

The heater case provides thermal insulation, neutral buoyancy, and protection for the heater components. It is constructed of syntactic foam sandwiched between inner and outer fiberglass shells. The foam provides buoyancy and thermal insulation, while the fiberglass provides mechanical strength. Overall wall thickness for the case is 5/8 inch on two sides and top and 3/4 inch on the two remaining sides. Heat loss through the case walls with a 106^{o}F (59^{o}C) temperature differential was found to be approximately 90 watts.

The case is built in two separate sections (Figure 22). The upper case contains the heat source, electrolyte, electrolyte/suit-water heat exchanger, hydrogen vent valves, and an economizer heat exchanger. The lower case houses the pumps, motors, monitoring electronics, and interconnecting plumbing. The upper case is sealed, while the lower case is free-flooding.

The seal between the upper case and the environment is an O-ring placed against a flat rubber gasket. Sealing pressure is provided by six plastic cam latches. The overall outer dimensions for the 8-kW-hr case are 8 x 8-1/2 x 14-1/2 inches (20 x 22 x 37 cm). The case weighs 11 pounds (5 kg). The 16-kW-hr heater measures 7-1/4 x 7-1/2 x 21-3/4 inches (18 x 19 x 55 cm).

Heat Production System

The heat source, which weighs 10 pounds (4.5 kg), consists of a series of cells (Figure 2) bolted (shorted) together. Twenty magnesium anodes 5-7/8 x 7-3/8 x 1/8 inch thick (14.9 x 18.7 x 0.32 cm) and 21 steel cathodes 0.010 inch (0.026 cm) thick are spaced at an electrode gap of 0.060 inch (0.152 cm). The electrode gap is fixed by copper spacer washers that also serve as electrical current paths between adjacent electrodes. Copper washers are used to minimize local reaction on the anode.*

With the above cell construction the starting power density in 140°F (60°C) electrolyte is approximately 1 W/in.^{2} of magnesium surface area (0.155 W/cm^2), which gives a total initial power for this cell of 1,800 watts. At the end of 8 hours, the power density decays to about 0.6 W/in.^{2} (0.093 W/cm^2), which provides the required 1,000 watts. The decay is primarily due to increased electrode gap resulting from anode consumption.

An important part of the heat production system is maintenance of the electrolyte and disposal of reaction products. Hydrogen must be continuously vented to prevent overpressurizing of the case. The hydrogen vent system is designed to provide an electrolyte overpressure of 1 psi (6.9 kPa) that is used to expel the spent electrolyte slurry at a rate of 0.026 gal/min (100 ml/min) through the economizer. Since the diver's orientation is constantly changing, the gas vents must be located on all corners of the case. In this model, the hydrogen vents are relief valves that are set at 1 psi (6.9 kPa) over ambient and are equipped with neutrally buoyant rubber flapper valves (Figure 24). In the presence of hydrogen, the flappers open, which allows the gas to escape through the relief valve. With water present, the flappers close to prevent hot electrolyte from being expelled to the environment.

A hydrogen-permeable membrane was explored for ventilating the hydrogen. Nonwettable porous Teflons and other synthetic materials were tested. The porous Teflon adequately vented the hydrogen with the required overpressure in clean seawater, but it was subject to pore clogging in the presence of magnesium hydroxide. Further investigation is necessary to find a noncloggable hydrogen-permeable membrane.

The economizer heat exchanger (Figure 25) is mounted within the two thick sides of the heater case. The seawater/magnesium hydroxide slurry passes through the copper tubing. The 0.18-inch (0.46-cm) inside diameter and the 17-foot (5.2-in.) length of the tubing were sized to provide a continuous discharge of 9.5 cu in./min [(150 ml/min)

*Local reaction around similar steel washers causes the anodes to prematurely corrode through, which separates the main portion of the anode from the short circuit paths.

at the 1-psi (6.9-kPa) hydrogen overpressure. Fresh seawater is pumped, counter flow, through milled channels surrounding the copper tubing. The rate is slightly greater than the slurry expulsion rate to provide for water consumed by the reaction. The entering fresh seawater is preheated by the expelled slurry. Tests of the economizer showed it to be approximately 75% effective in recovering heat from the spent electrolyte.

Heat Circulation System

Heat is distributed to the diver by means of a second fluid (seawater) that is circulated through a heat distribution garment surrounding his body. A schematic of the system is shown in Figure 23. The pump circulates water at a rate of 0.6 gal/min (2.27 ℓ/min) through the semi-closed circuit loop. As this fluid passes through the electrolyte-immersed heat exchanger, its temperature is raised to approximately 115°F (46°C). A piston-type thermostatic actuator, which is mounted in the temperature control valve (Figure 26), senses the temperature of the water delivered from the heat exchanger. The position of the thermostat is set so that if the temperature exceeds 110°F (43°C), the piston will open a throttling valve that will allow the hot water to escape to the sea.

An equal volume of cold seawater is automatically taken in through the always-open suction port at the pump. The cold water mixes with the warm water returned from the diver before entering the heat exchanger, and lowers the temperature of the water delivered to the diver. A handle on the valve allows the diver to adjust the set point position of the thermostat. With this handle the diver suit water inlet temperature is adjustable for comfort control. By opening the valve, the diver can bypass some or all of the heated water and circulate cool water through the suit. The high temperature set point can be adjusted to a maximum of 110°F (43°C).

System Components

The pumps for circulating the diver suit water and fresh electrolyte are shown in Figure 27. The permanent magnet DC motors are housed in watertight pressure vessels. To avoid the need for shaft seals, magnetic couplings are used to drive the centrifugal pump impellers. The pumps are activated by an electronic control panel (Figure 27) that also monitors the system. The control panel contains three sets of LEDs* which, when lighted, give the diver the following information:

*Light emitting diodes.

1. Low pump current (pump cavitating)

2. Suit water temperature too high [>110°F (43°C)]

3. Cell temperature below 140°F (60°C)

The control panel also contains two off/on switches — a diver-operated one for suit circulation, and another one for activation of the electrolyte pump and electronics. Thermistors sense the cell and suit-water temperatures. The electronic components are housed in a watertight pressure housing attached to the pump motors. The electronic/electrical control circuit is shown in Figure 28.

Power for operating the pump motors and electronics is supplied from three parallel sets of four D-size lithium primary cells connected in series to provide 10.5 volts and 17 A-hr. The batteries are contained in watertight housings (Figure 29) that are mounted external to the heater case.

Safety Considerations

Safety is an inherent characteristic of the heat source; the reaction produces no toxic substances, and the high reaction temperatures that might result from overheating are limited to the local boiling point of seawater. If the temperature of the electrolyte exceeds 140°F, which could occur if the diver load were to be less than the anticipated 1,000 watts, the electrolyte/suit-water heat exchanger will transfer the additional heat to the diver circuit and elevate the suit-water temperature. This immediately activates the temperature control valve, which causes the hot water to be dumped and cold water to be taken in at the circulation pump. The incoming cold water creates a load that exceeds the capacity of the cell, thereby causing a subsequent reduction in the electrolyte temperature. As an additional thermal safety device, if an excessive electrolyte temperature were to occur, the extra hydrogen produced would cause a higher internal case pressure and subsequent dewatering of the cell.

By adjusting the temperature control valve, the diver can automatically control the temperature of his suit water at any point within the 100°F-to-110°F (38°-to-43°C) range. If the diver sets the valve below the automatic control range, he can dump any portion or virtually all of the heater output and circulate cool water through the suit. If the temperature control valve should fail, the diver could remain comfortable by periodically connecting and disconnecting couplings in the suit-water hoses. The only possible hazard from the heater is the accumulation of an explosive concentration of hydrogen if the heater is operated in a closed space for a prolonged period of time.

Heater Testing

Laboratory bench tests of the heater were conducted to determine overall performance. Electrolyte temperature, temperatures across the diver load, and suit-water flowrate were recorded. The diver load was simulated by immersing a copper tubing heat exchanger into a refrigerated bath. The heater's power output was calculated using the flowrate and the suit-water temperatures. A typical power curve for an 8-hour test is shown in Figure 30. Power output for the 16-kW-hr heater is shown in Figure 31.

In late May 1975 the heater was first integrated with the heat distribution garment and thermal protection suit developed by NCSL. Previous tests with a diver had established a base line power requirement and typical skin and rectal temperature trends.

For the integrated test, the heater was carried on the diver's back and suit-water flow and electrolyte and suit-water temperatures were monitored. The diver's rectal temperature was used as the absolute indicator of the heater's effectiveness. During the first 4 hours of the test, the rectal temperature exhibited the typical slow decline. However, just after 4 hours, it began to rise (Figure 32) and continued to rise during the next hour. The test was considered successful since the temperature rise indicated that the diver was returning to a stable, normal condition.

Human Considerations

Since the end product of this development effort will be hardware carried by free-swimming divers, a human factors study was initiated to determine man/equipment interface problems (the appendix). The objective of the study was to determine what size and shape the heater could attain without restricting the free-swimming diver's mobility. Discussions were held with cognizant tactical diver-oriented personnel, and then mock-ups of potential diver heating units based on available free-body space were built and tested. The testing involved diver/swimmer drag measurements and diver subjective analysis.

The results of the human factors analysis showed that a chest mock-up (Figure 33) was preferred over the others tested. The divers favored the chest-worn unit, because they would prefer to retain the heater and stay warm in the water if they should have to ditch their breathing equipment.

CONCLUSIONS

1. Laboratory and diver tests have proved the feasibility of the magnesium/seawater reaction for producing heat. Up to 2 kW of power have been produced continuously for 8-hour periods.

2. A reliable, safe, compact heater can be built that will supply the diver's needs in cold water.

3. The specific power output in terms of volume and weight is competitive with past developed and potential future heat sources.

4. Based on the results of laboratory and diver experiments, a neutrally buoyant, diver-carried, dual-plate heater can be expected to occupy a volume of approximately 143 $in.^3$/kW-hr (2,340 cm^3/kW-hr).

5. Since the requirements for heat will vary in accordance with other factors, such as depth, water temperature, and diving systems, it is expected that future heaters will be modular and will have variable power output and endurance.

6. In the case of the dual-plate heater cell it may be more practical to use a submersible- or diving-bell-mounted heater and supply the diver through a hot water umbilical; however, large heat losses in umbilical hoses could require the heater to be several times the size of that needed for actual diver use.

7. It is practical to consider using the magnesium/seawater reaction as an emergency heat source on submersibles or as a come-home heat source for divers. The system would be activated by charging it with seawater when heat is required.

8. The final location and configuration of the diver-carried heater will be determined by diver needs and breathing apparatus. For one Navy operation it was found that a chest unit mounted under breathing bags was most practical in terms of diver comfort and swimability. This unit could supply 2 kW-hr, would occupy a volume of 2 x 20 x 20 inches (5 x 15 x 15 cm), and would be neutrally buoyant.

9. For SDV-type* operations it would be practical to consider mounting the heater in the SDV instead of on the diver. A smaller, shorter duration heat storage or heat production pack could be carried by the diver for out of SDV operations.

---

*Swimmer Delivery Vehicle, a wet submersible.

10. The major problem yet to be resolved in the development of a free-swimming diver-carried dual-plate heater is the venting of hydrogen produced by the reaction. The vent system must be operable in virtually any orientation, while preventing excessive electrolyte leakage to sea. Operation of the vent system is further complicated by the clogging nature of the $Mg(OH)_2$ reaction by-products.

11. The alloyed magnesium-iron powders offer a viable solution to some of the undesirable characteristics of the dual-plate cells, including:

(a) Higher specific output than the dual-plate cell
(b) Constant or controlled power output
(c) Attitude insensitive to venting of H_2
(d) Easily modularized to suit mission requirements

RECOMMENDATIONS

1. A plate-type (dual or iron-plated) magnesium-iron heater for use in limited orientation situations, such as mounted on a PTC, SDV or submersible, should be built and tested. This heater could also be used as a standby emergency heater for the same vehicles.

2. Additional test and evaluation of magnesium-iron powdered alloys, including other cathodic materials, should be conducted. Based on the results of these tests, a portable diver-carried heater with constant or variable power output should be designed, fabricated, and tested.

REFERENCES

1. Naval Medical Research Institute. Report no. 2: Theoretical thermal requirements for the Mark II diving system, by J. F. Tauber, J. S. P. Rawlins, and K. R. Bondi. Bethesda, Md., 1969. (AD 694013)

2. Naval Coastal Systems Laboratory. Informal Status Report: Thermal comparison of various diver suit materials, by R. K. Johnson. Panama City, Fla., Mar. 1973.

3. Navy Experimental Diving Unit. Report no. NEDU-RR-3-51: Test of electrically heated clothing, by T. N. Blockwick. Washington, D. C., Feb. 1951. (AD 731013)

4. Naval Civil Engineering Laboratory. Technical Note N-1015: Marine Corps diver's backpack battery assembly, by D. Taylor and J. J. Bayles. Port Hueneme, Calif., Jan. 1969.

5. Naval Medical Research Institute. Report no. 1: Evaluation of Marine Corps battery powered electrically heated diving dress, by W. E. Moritz and H. C. Langworthy. Bethesda, Md., June 1972. (AD 749847)

6. ————. Report no. 8: Thermal protective suits for underwater swimmers, by E. L. Backman. Bethesda, Md., July 1966.

7. Naval Civil Engineering Laboratory. Technical Note N-1087: SEALAB III-Divers' isotopic swimsuit heater system, by J. J. Bayles and D. Taylor. Port Hueneme, Calif., May 1970. (AD 708680)

8. Naval Missile Center. Technical Memorandum TM-67-1: Timed heat-release chemical system for underwater applications, by K. N. Tinklepaugh and C. J. Crowell. Point Mugu, Calif., Feb. 1967.

9. Naval Civil Engineering Laboratory. Technical Note N-1108: Heat of crystallization as a heat source for divers, by P. J. Hearst. Port Hueneme, Calif., June 1970. (AD 873143L)

10. ————. Technical Note N-998: Chemical heat source for wet suits, by P. J. Hearst. Port Hueneme, Calif., Nov 1968. (AD 844923L)

11. Naval Ship Research and Development Laboratory. Report on Task WR-1-5118: Initial test and evaluation of CONOX diver heater, by H. S. Butler. Panama City, Fla., 1971.

12. Naval Civil Engineering laboratory. Technical Note N-1315: Preliminary development of an electrochemical heat source for military diver heating, by S. A. Black, et al. Port Hueneme, Calif., Nov. 1973. (AD 773065)

13. J. S. Benjamin and T. E. Volin. ''The mechanism of mechanical alloying,'' Metallurgical Transactions, vol. 5, no. 8, Aug. 1974, pp. 1929-1934.

14. J. S. Benjamin. ''Dispersion strengthened superalloys by mechanical alloying,'' Metallurgical Transactions, vol. 1. no. 10, Oct. 1970, pp. 2943-2951.

THE MAGNESIUM - SEAWATER REACTION

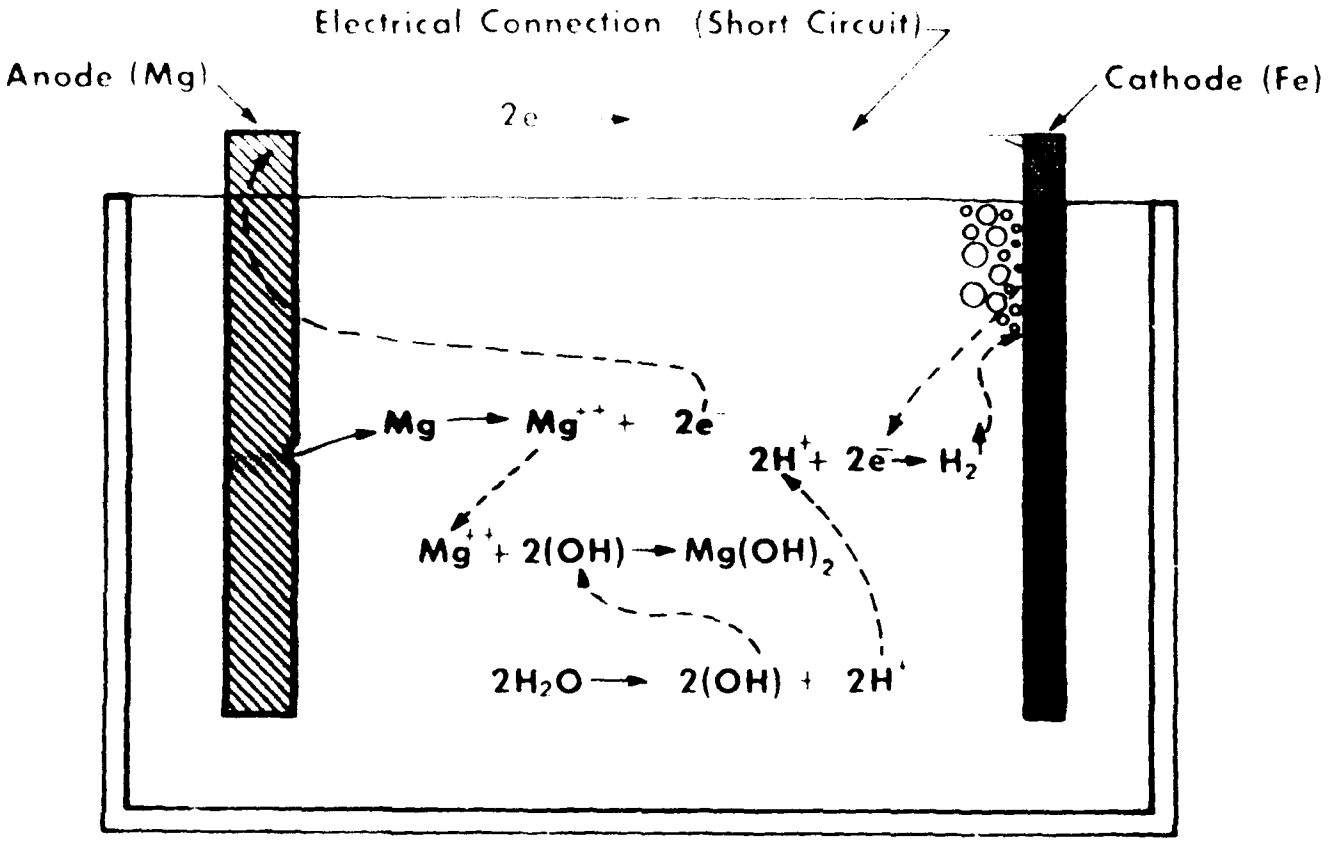

Figure 1. Schematic of the magnesium cell showing the primary reaction.

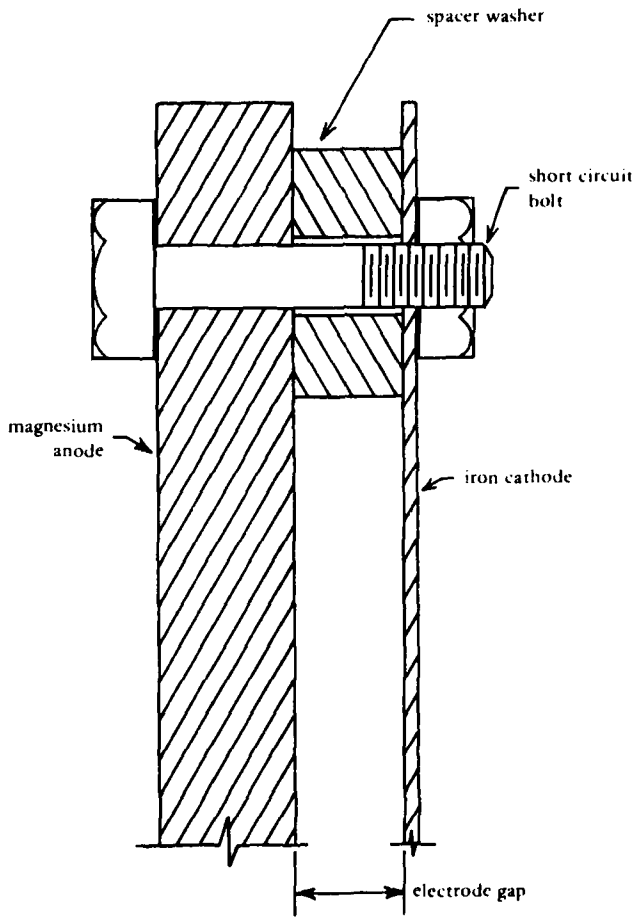

Figure 2. Dual-plate cell configuration.

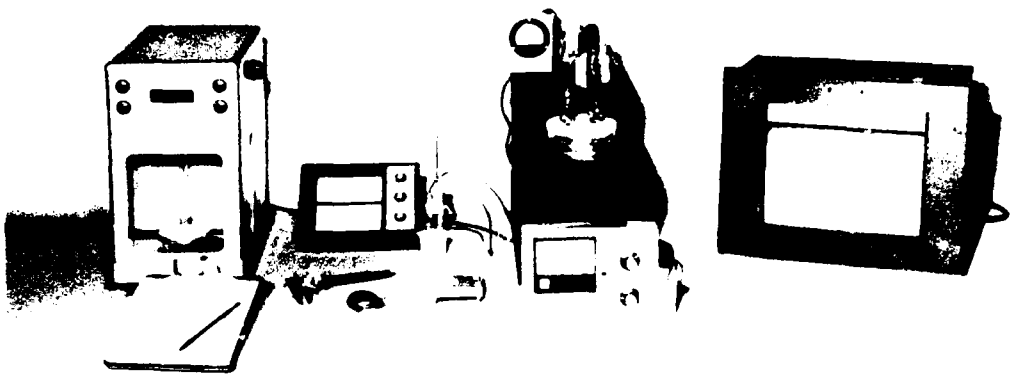

Figure 3. Dewar flask apparatus for parametric tests.

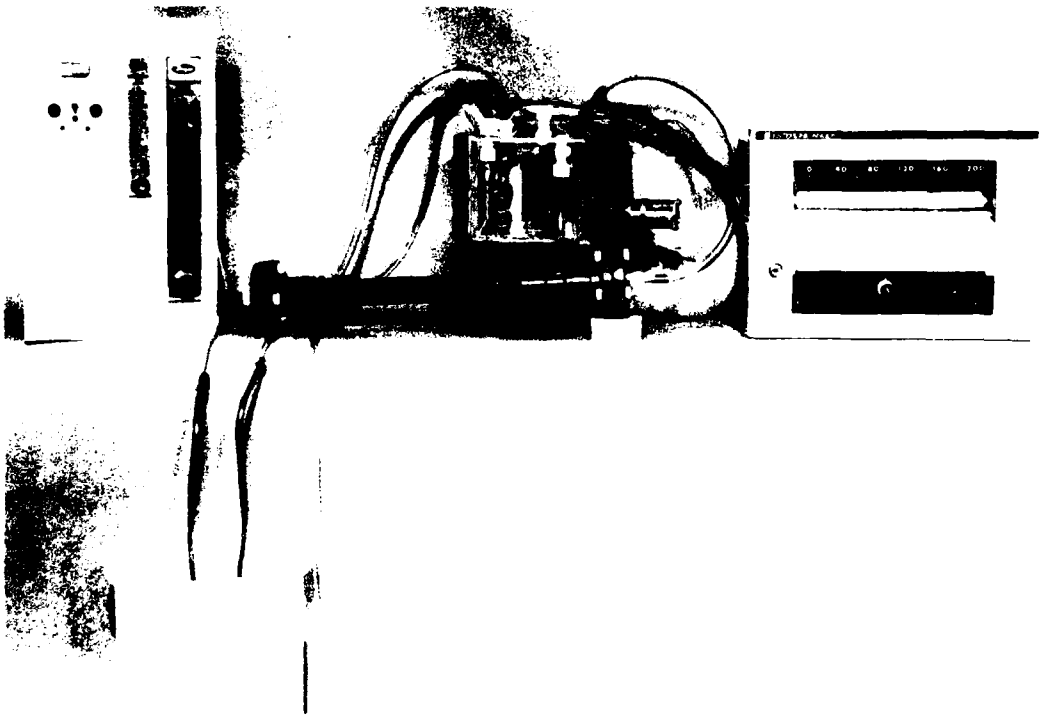

Figure 4. Acrylic vessel for large-scale 1,000-watt tests.

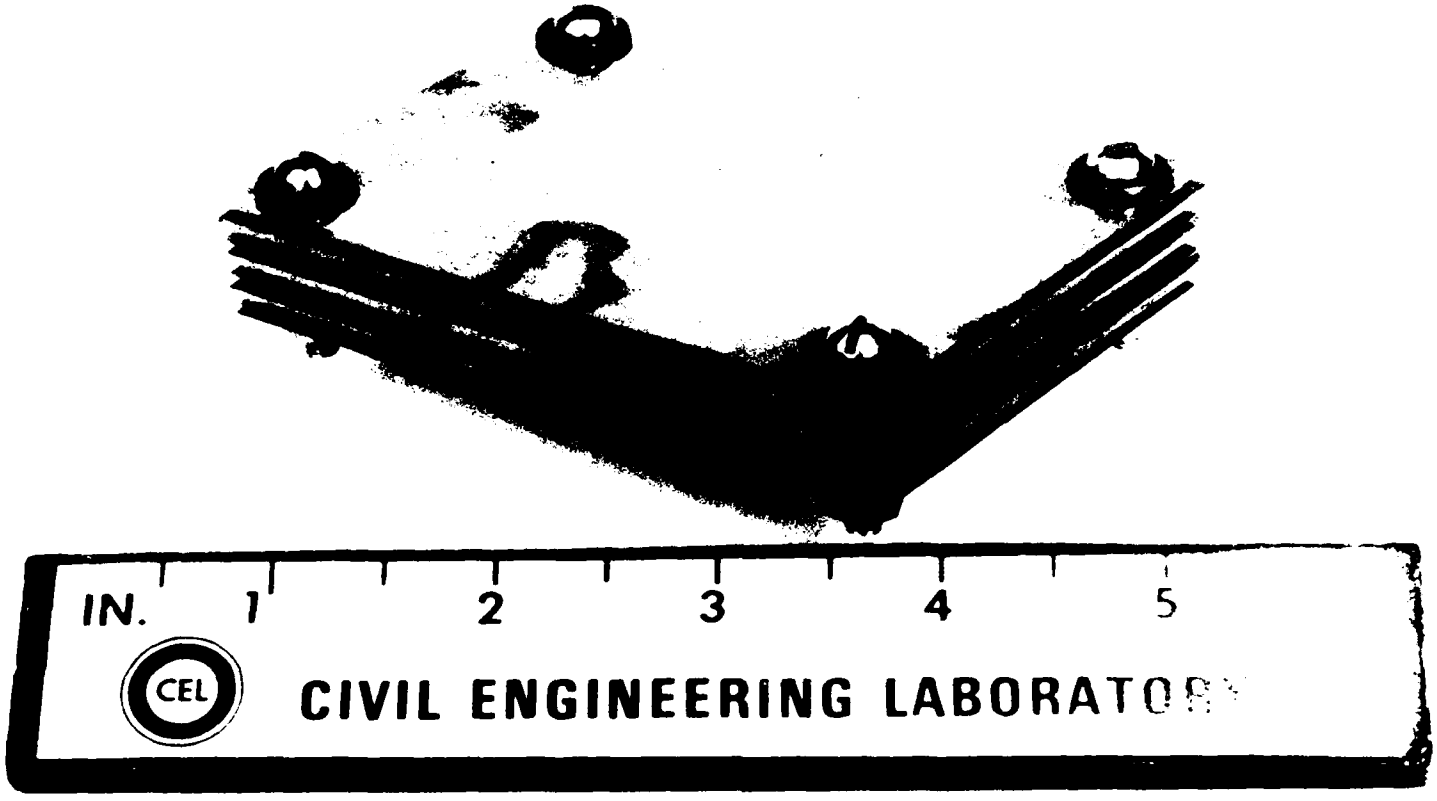

Figure 5. Typical dual-plate cell arrangement with three anode and four cathode plates.

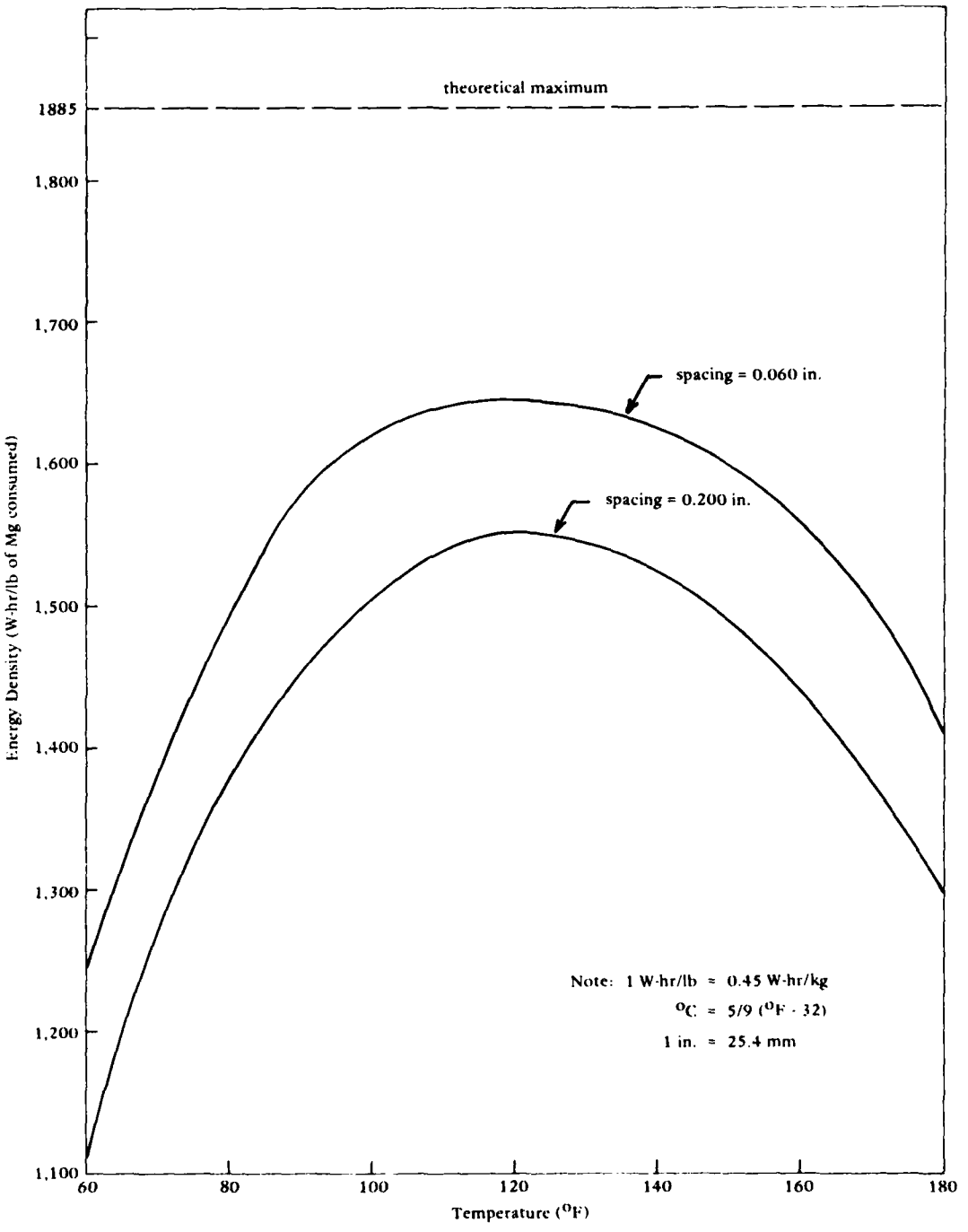

Figure 6. Energy density as a function of electrolyte temperature (for 0.060 in. $\leq$ spacing $\leq$ 0.200 in.).

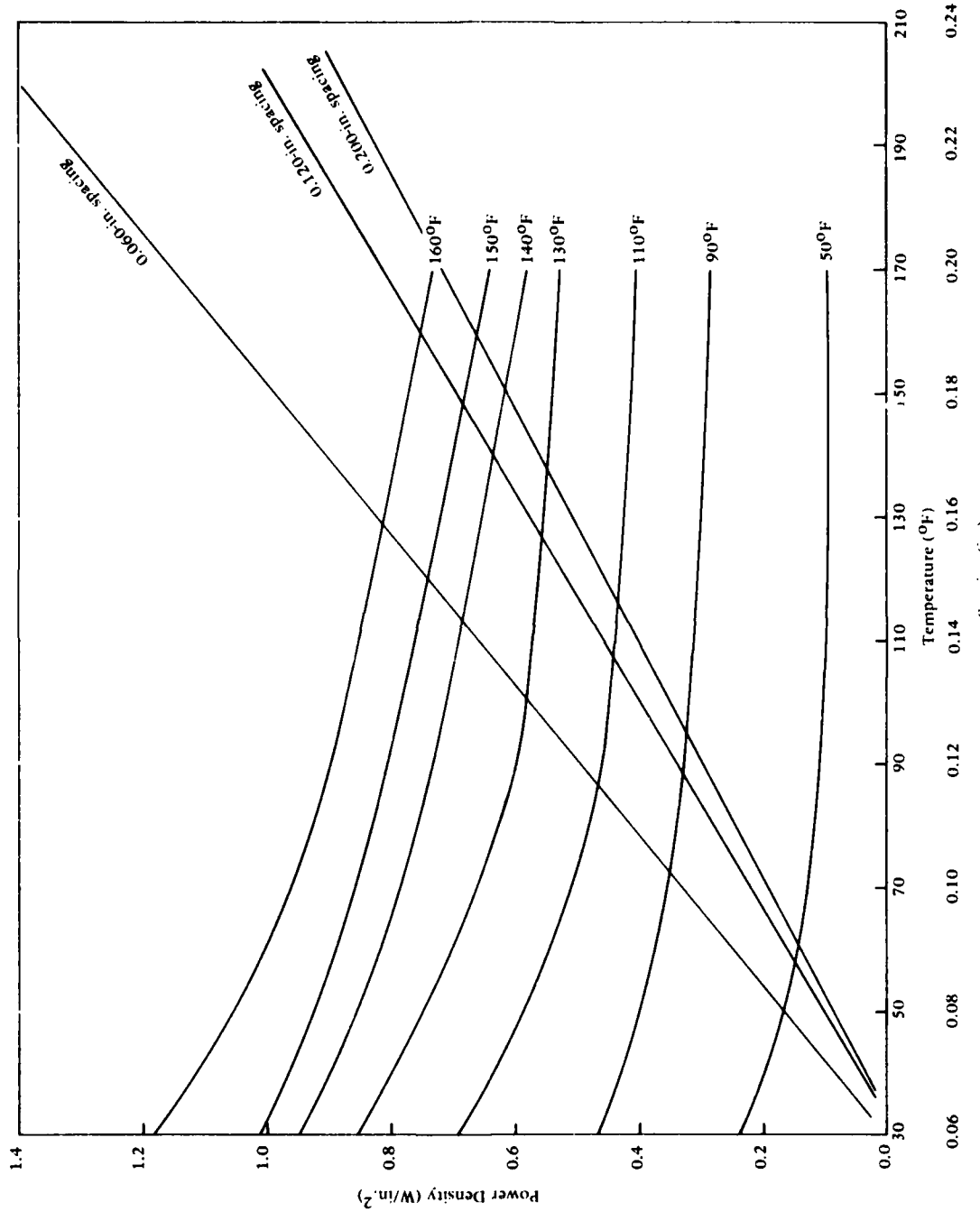

Figure 7. Power output as a function of plate spacing and electrolyte temperature.

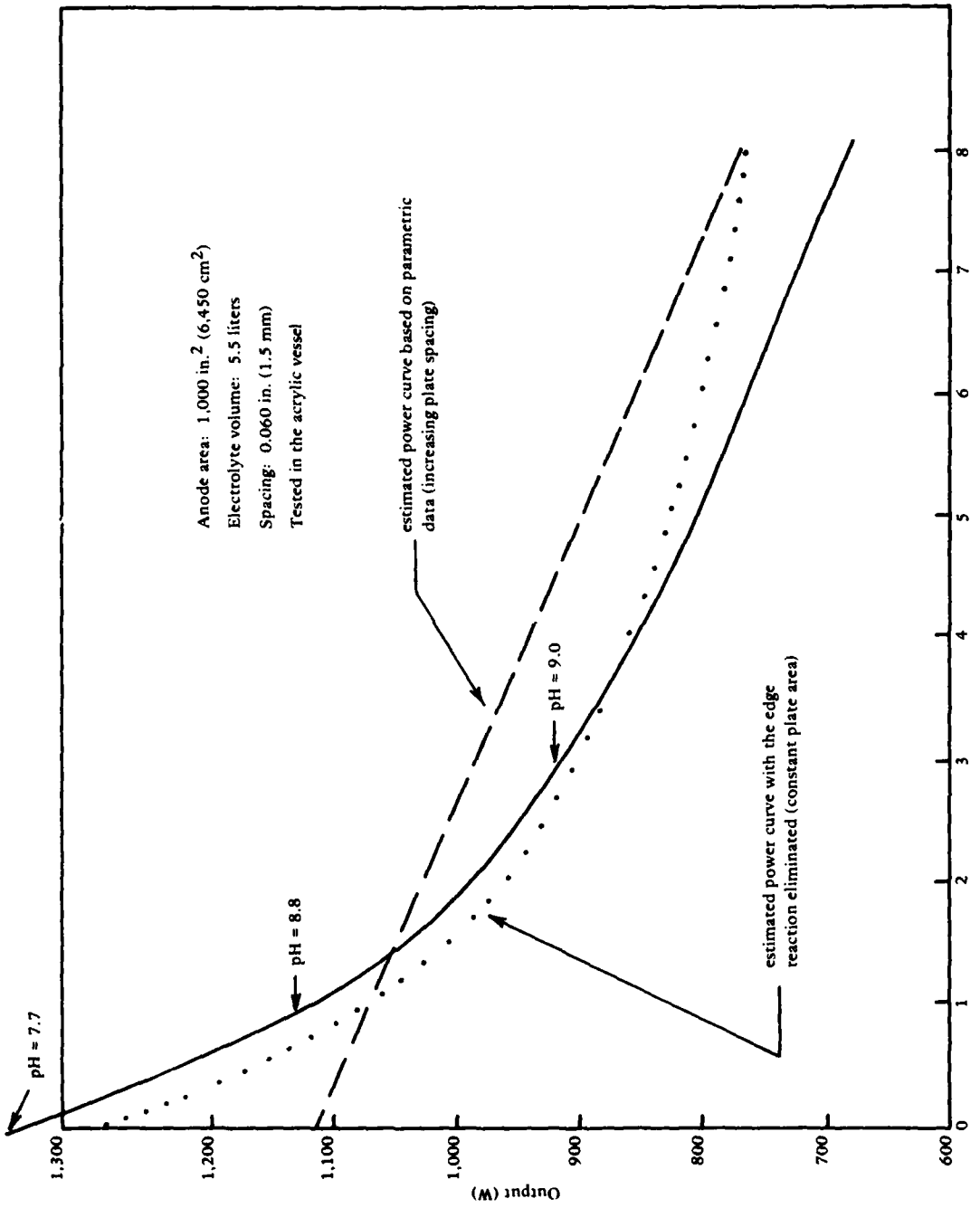

Figure 8. Reaction rate decay characteristics.

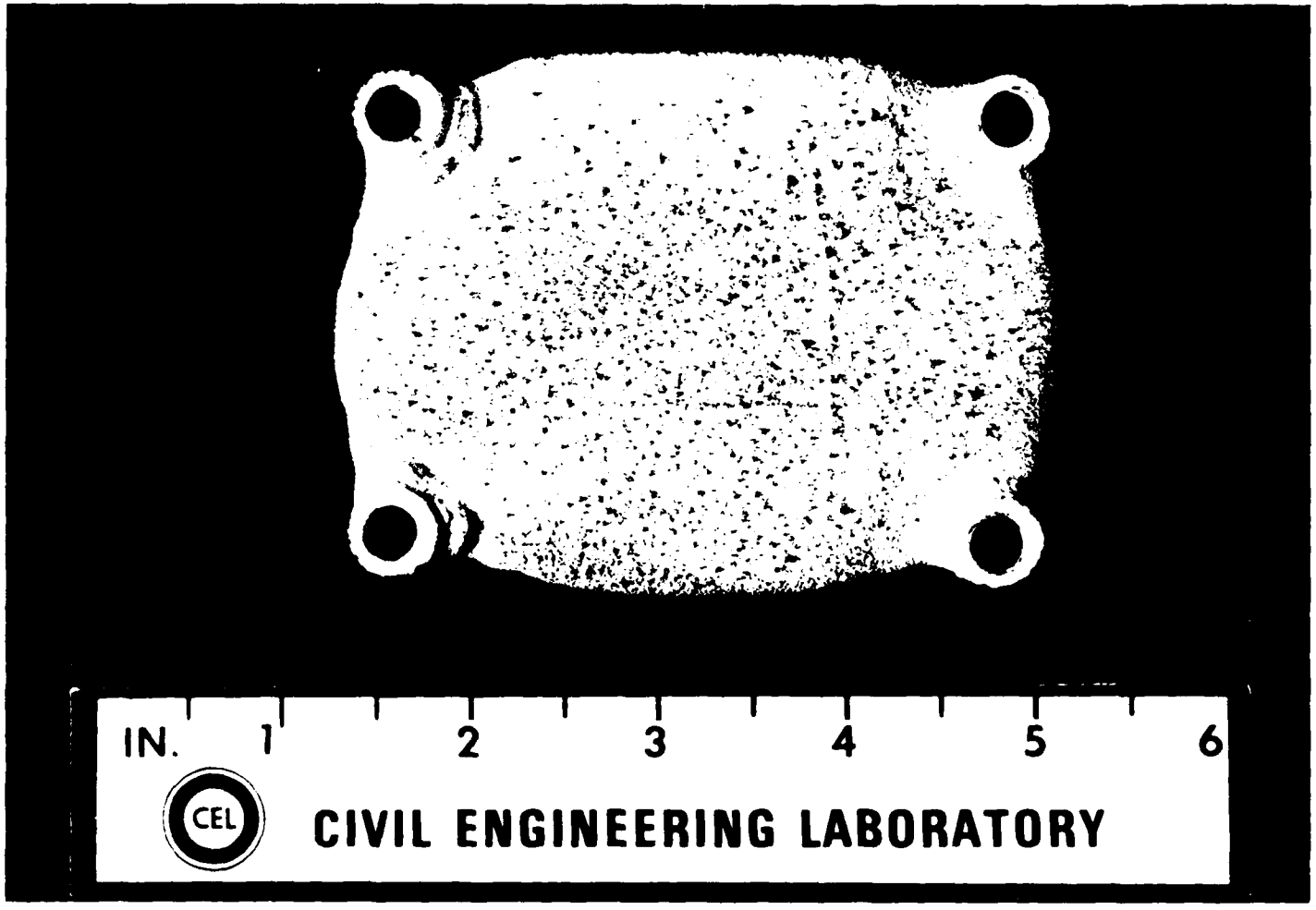

Figure 9. Magnesium anode showing diminished edge areas (original anode was 3 x 4 inches).

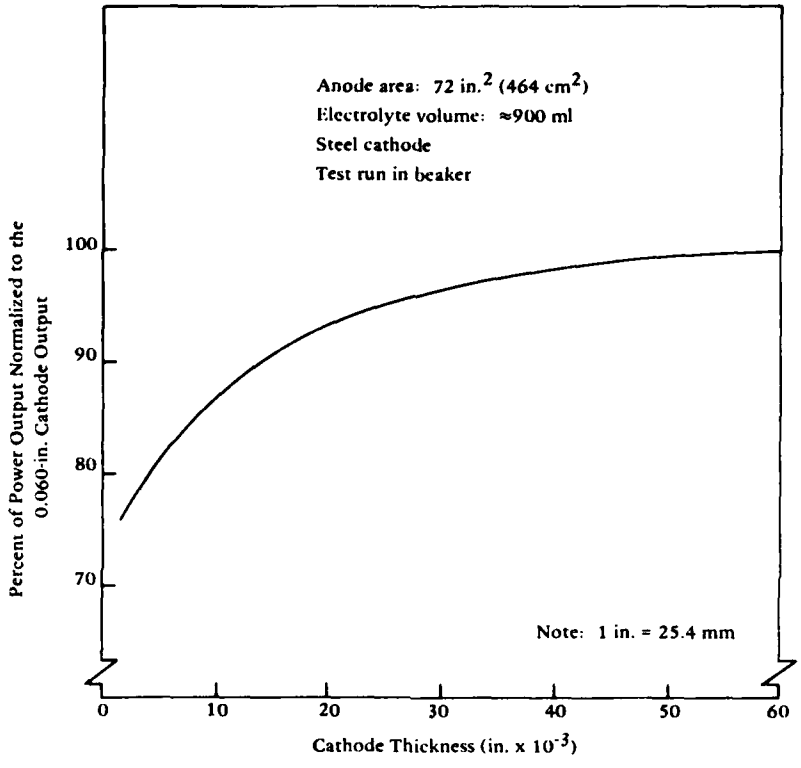

Figure 10. Cell output as a function of cathode thickness.

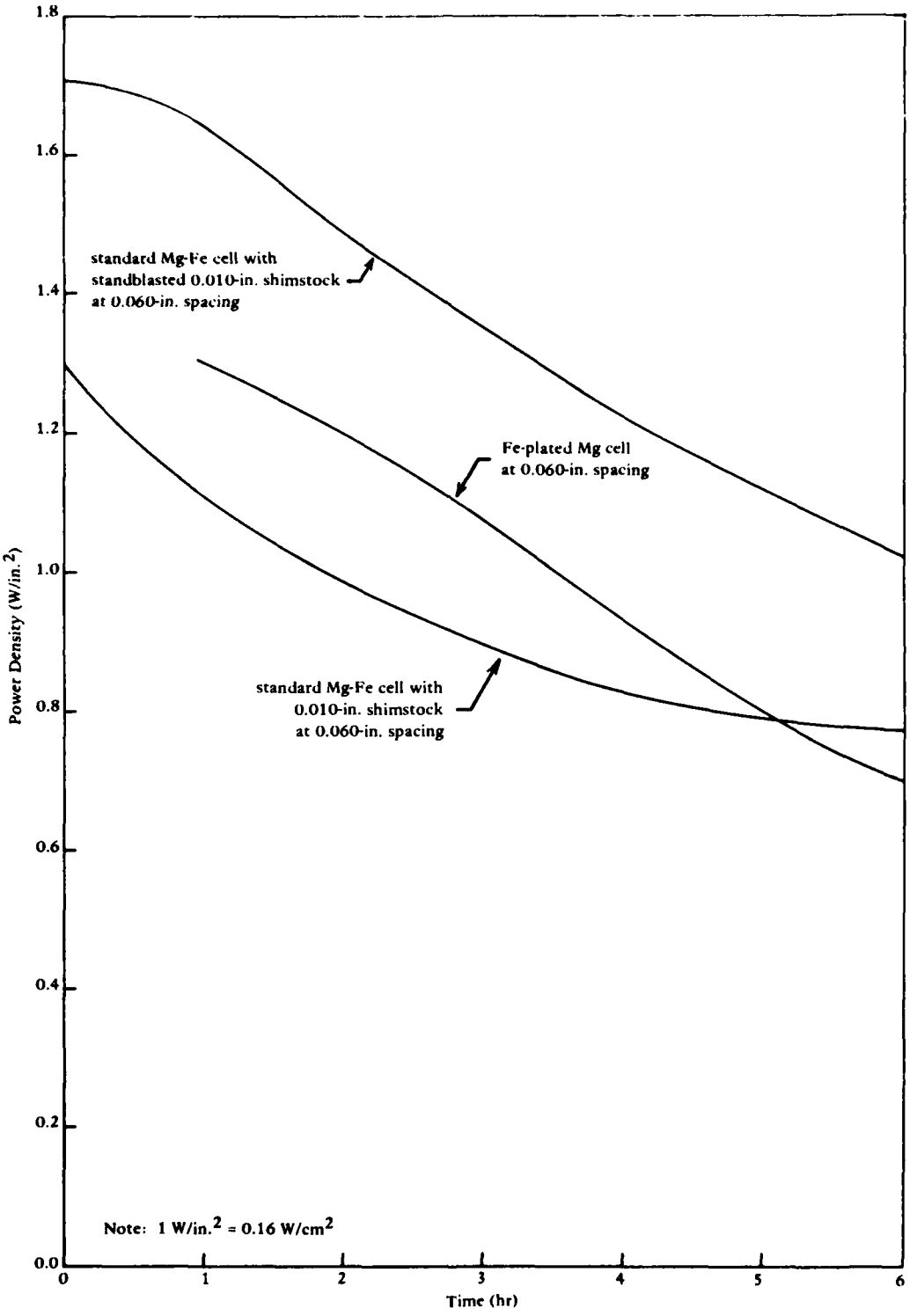

Figure 11. Bi-polar and sandblasted shimstock electrode test compared to dual-plate tests.

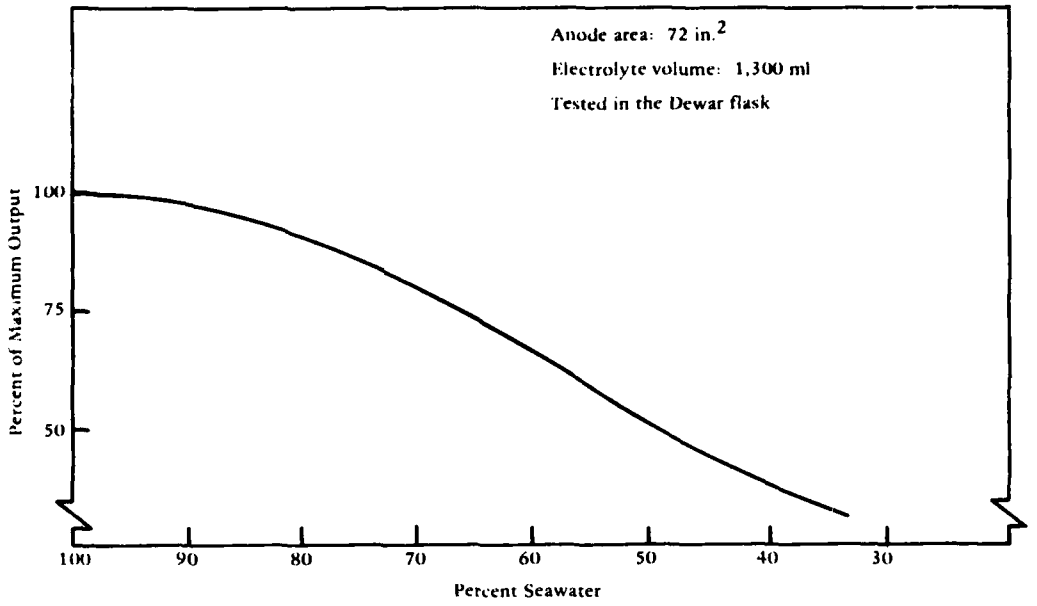

Figure 12. Cell output as a function of seawater concentration.

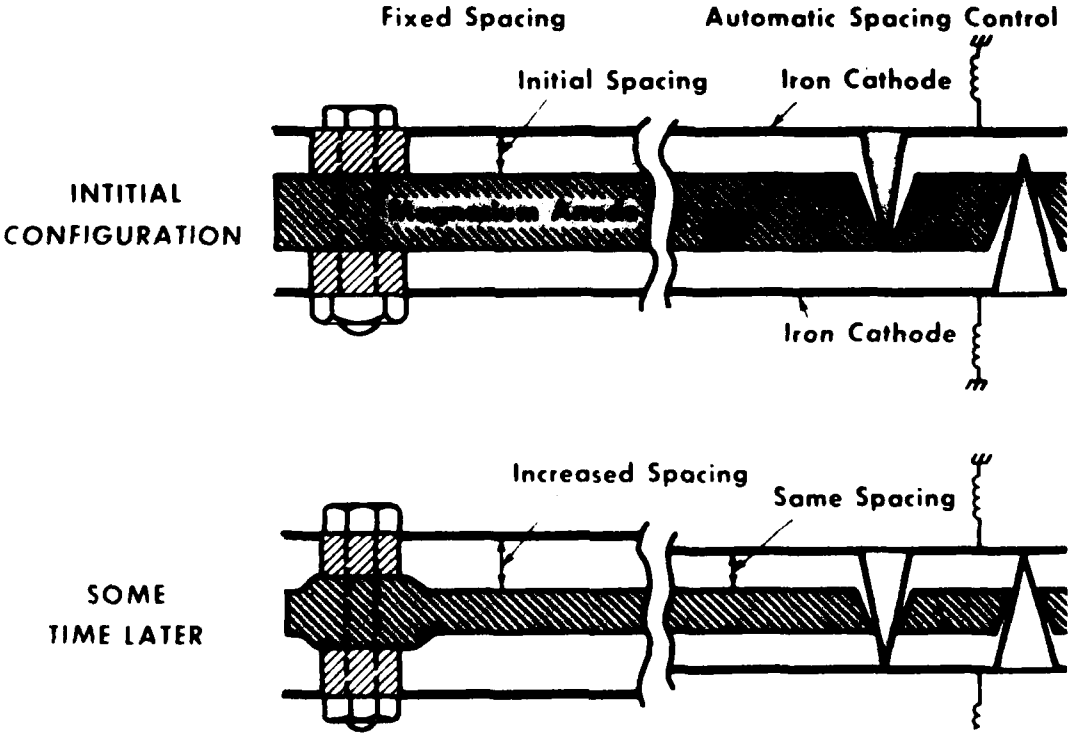

Figure 13. Inert cone spaces used for controlled-spacing tests.

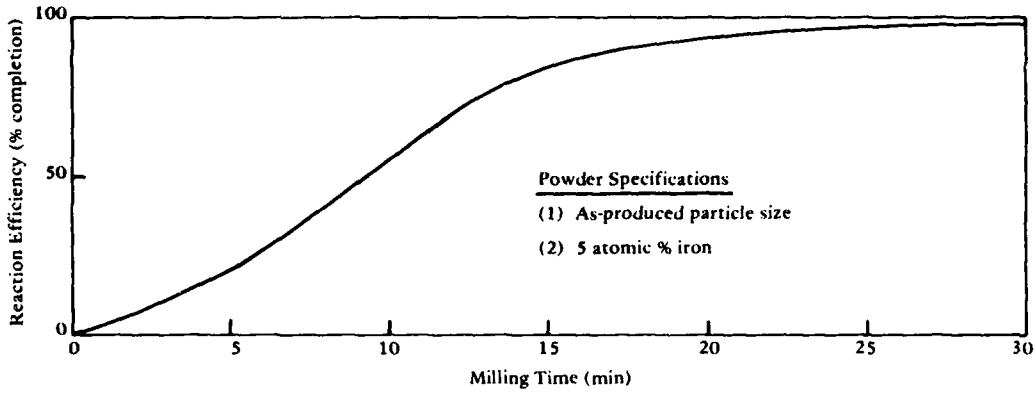

(a) Reaction efficiency versus milling time.

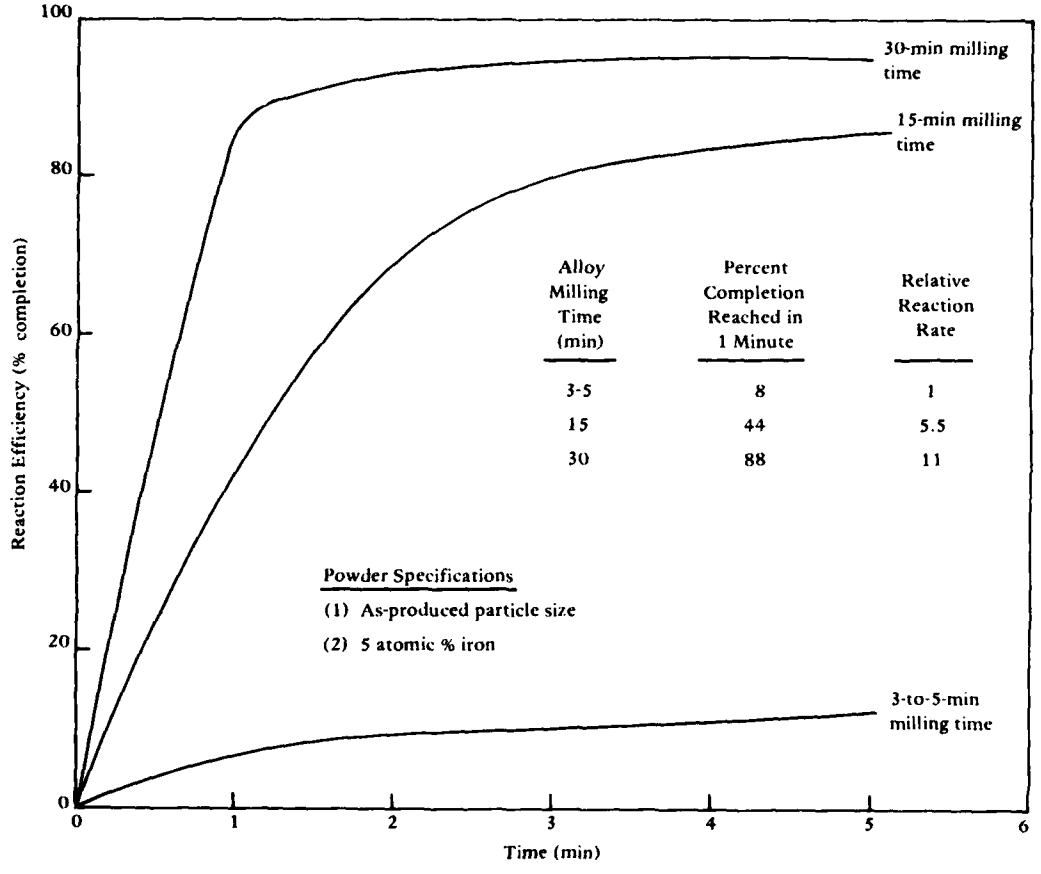

(b) Percent completion versus time.

Figure 14. Reaction efficiency as function of milling time.

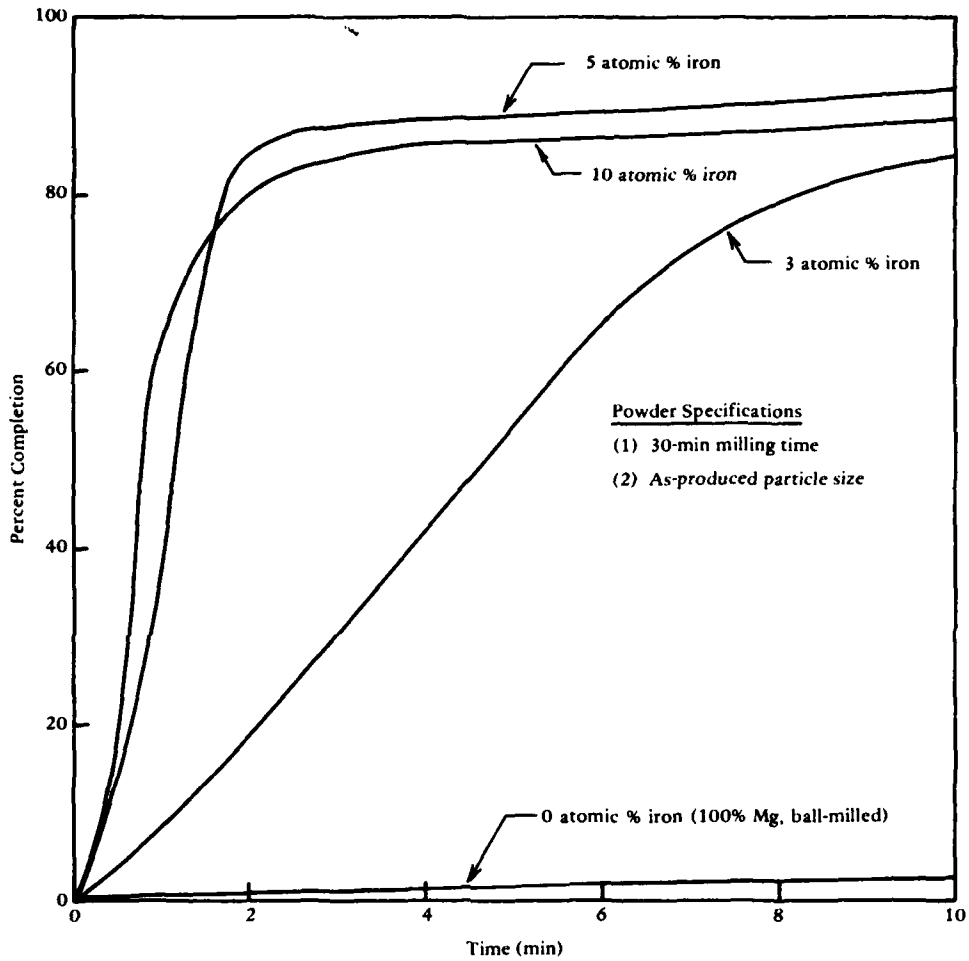

Figure 15. Effect of alloy composition on percent completion.

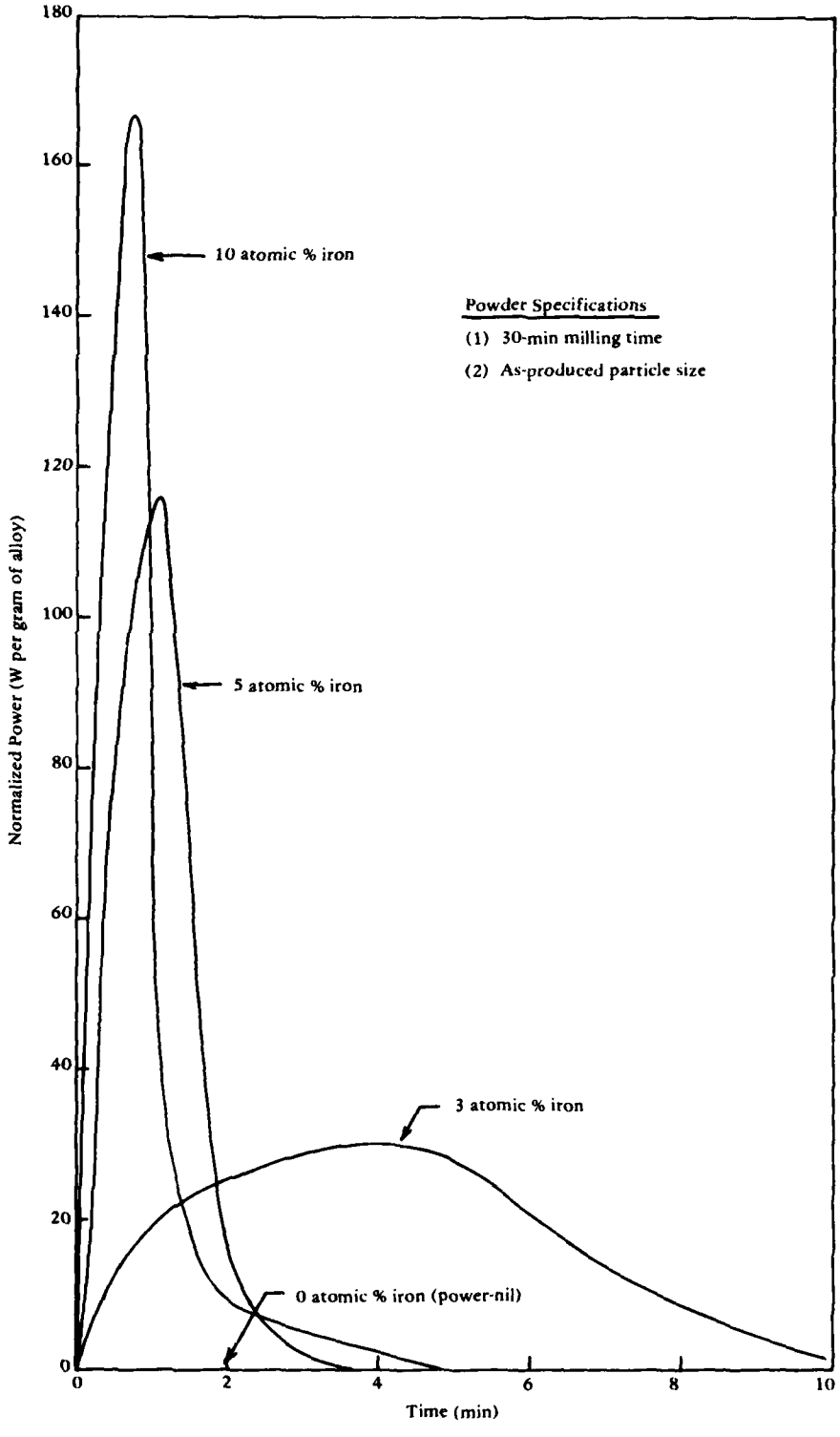

Figure 16. Power as a function of alloy composition.

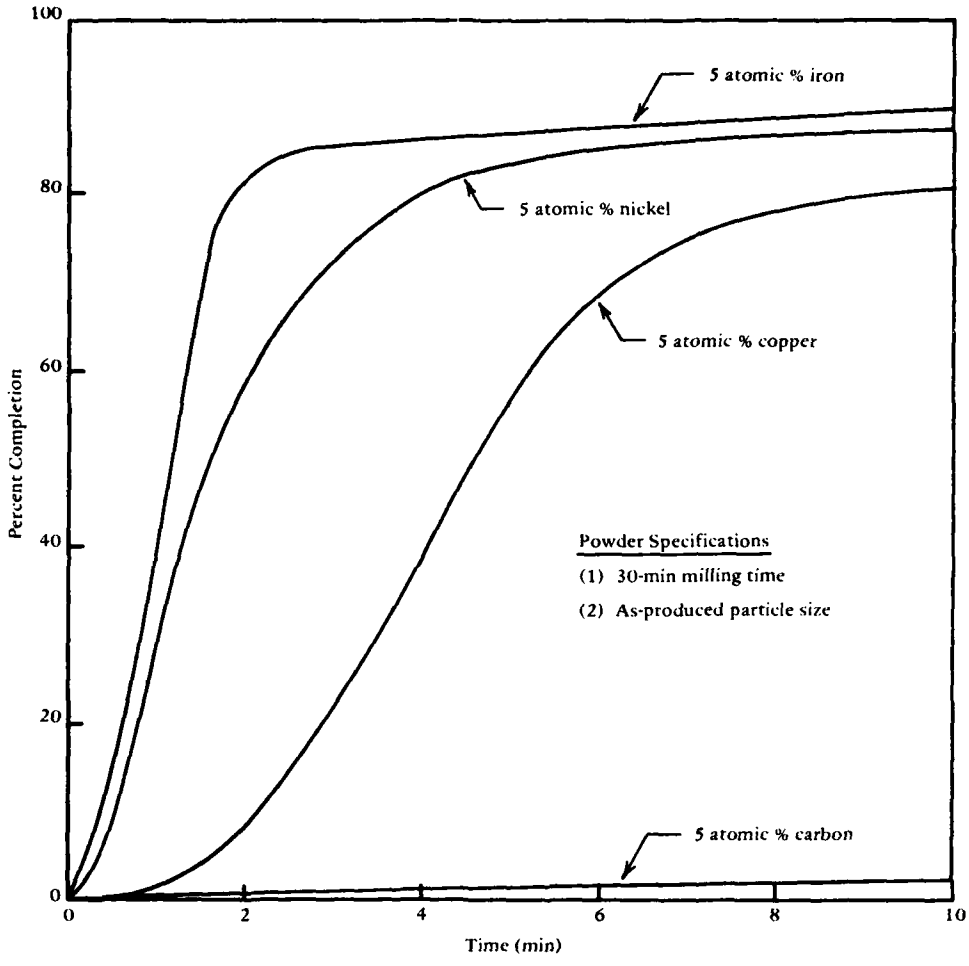

Figure 17. Reaction rates of alternate cathodic materials.

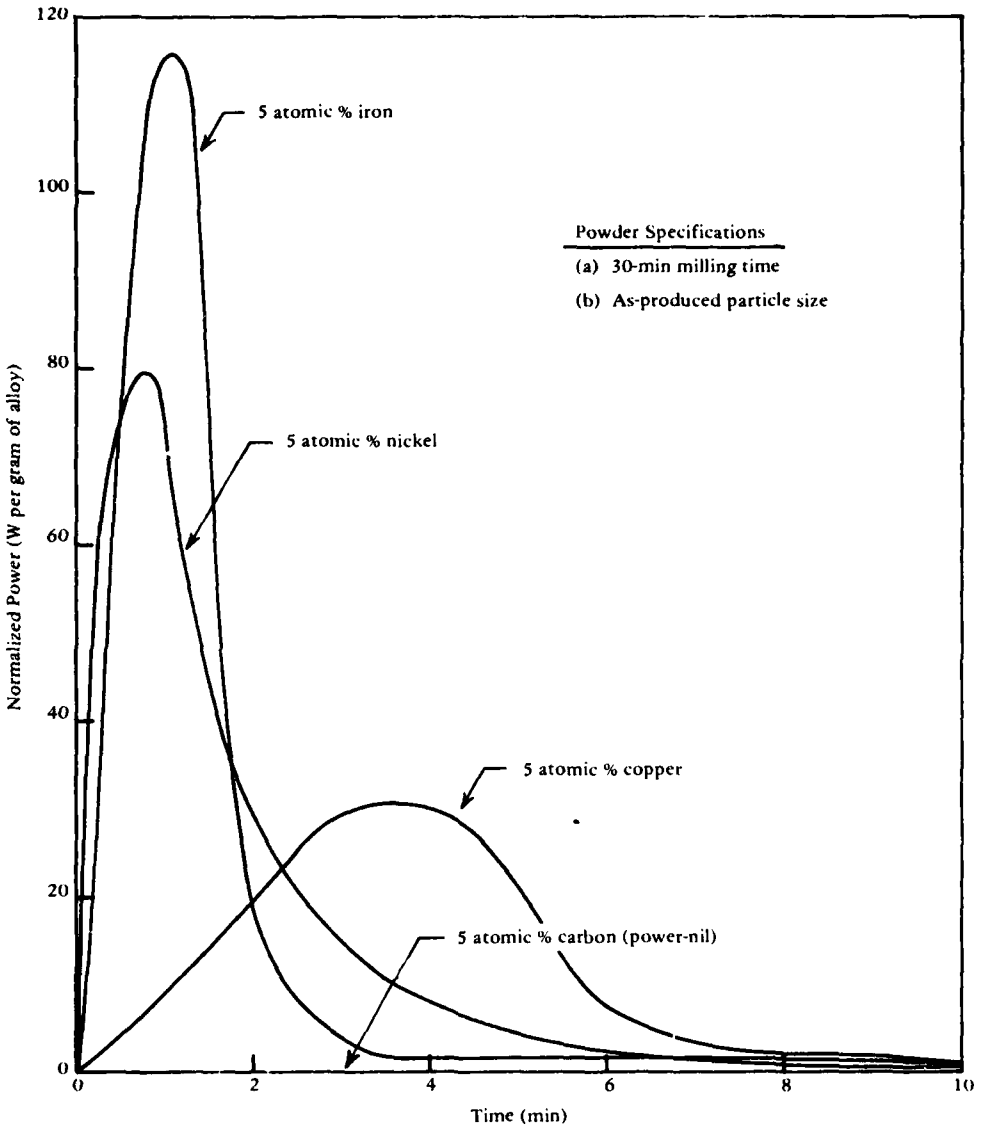

Figure 18. Power output for alternate cathodic materials.

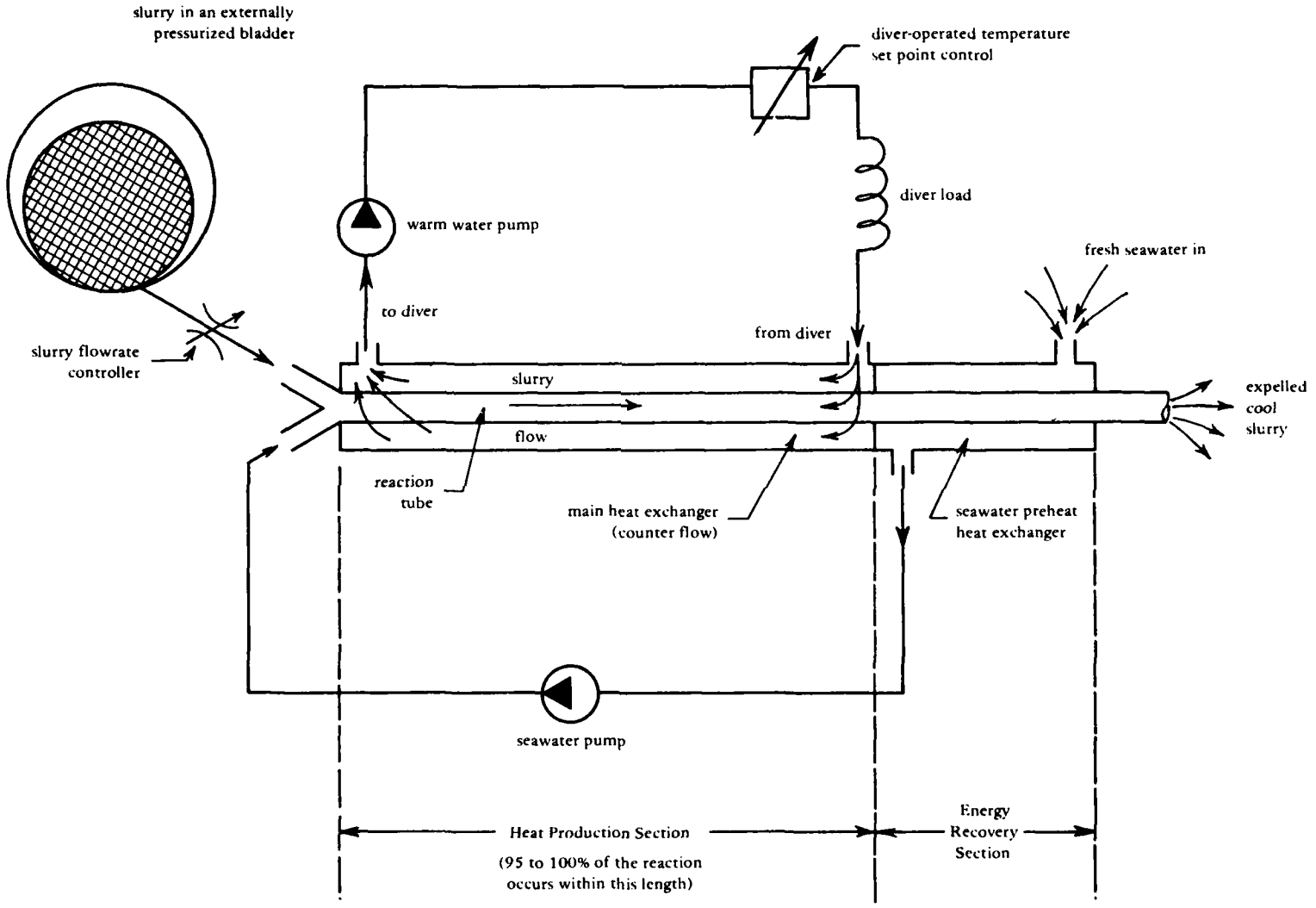

Figure 19. Schematic of powder alloy heater.

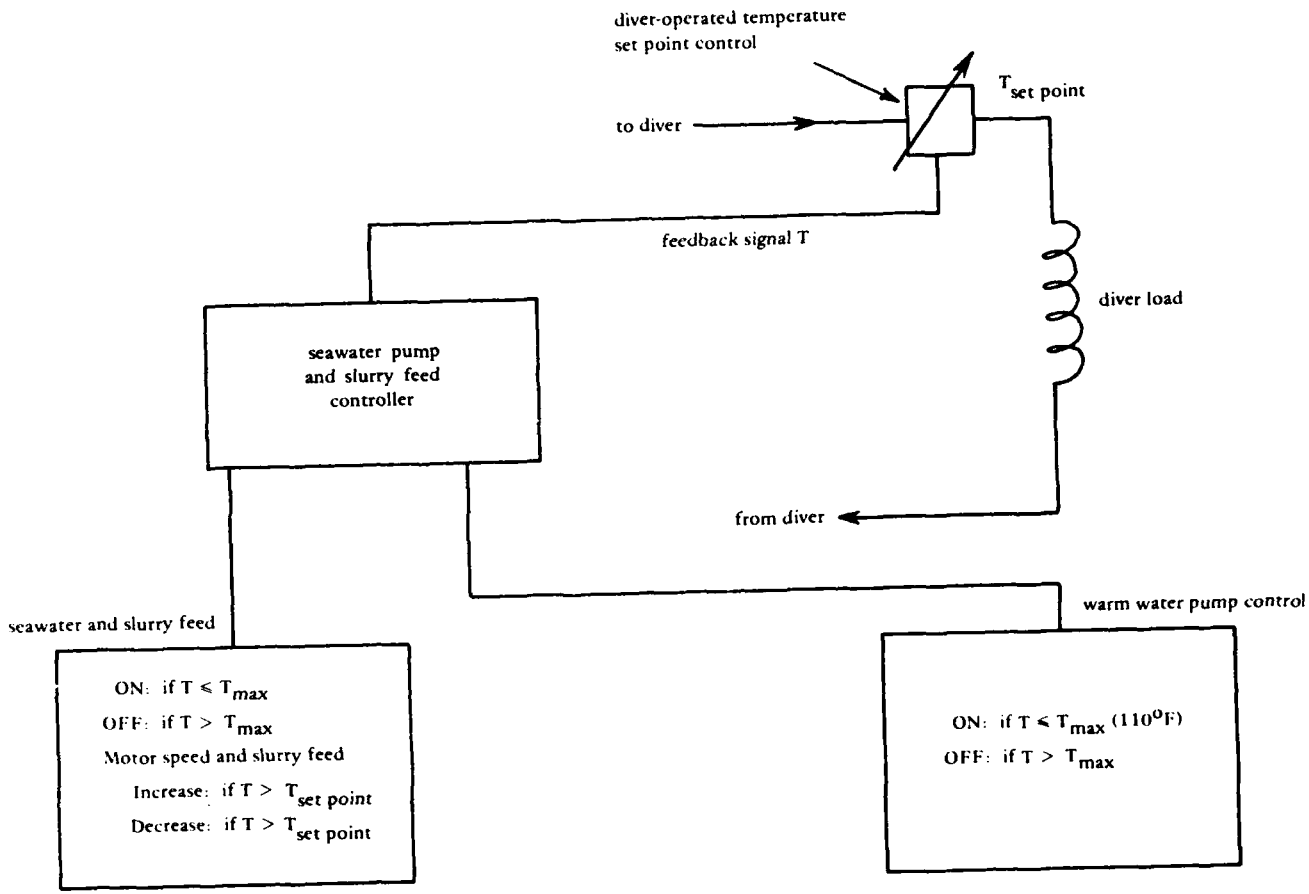

Figure 20. Control circuitry for powder alloy heater.

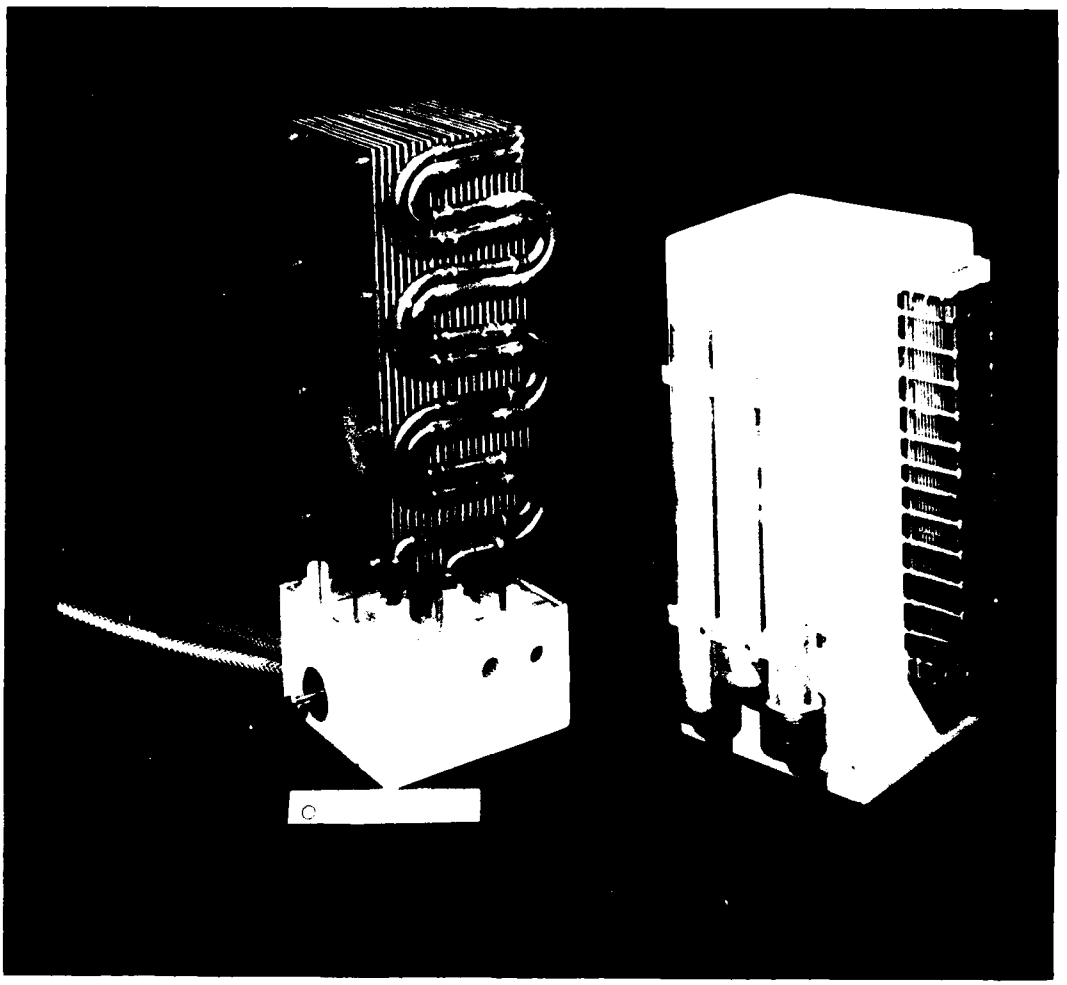

Figure 21. Experimental 16-kW-hr diver heater showing the magnesium-iron cell.

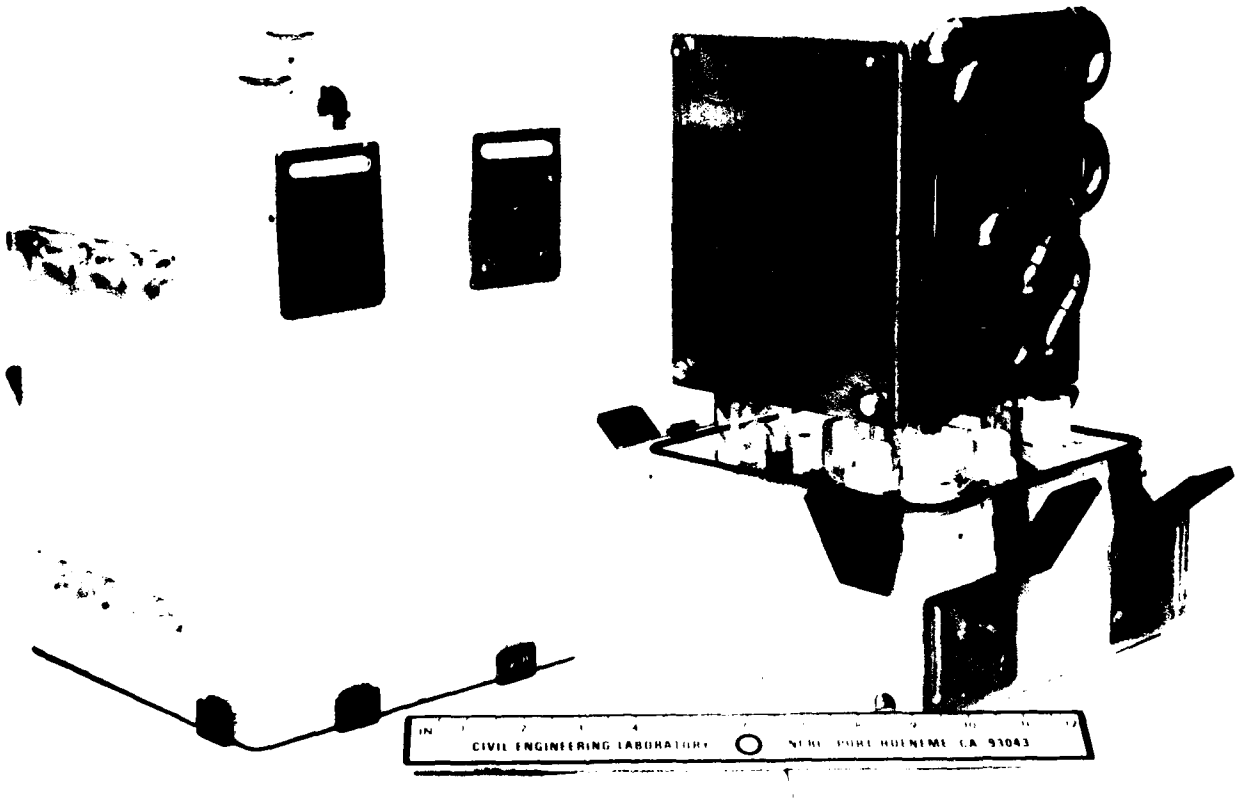

Figure 22. Experimental 8-kW-hr diver heater.

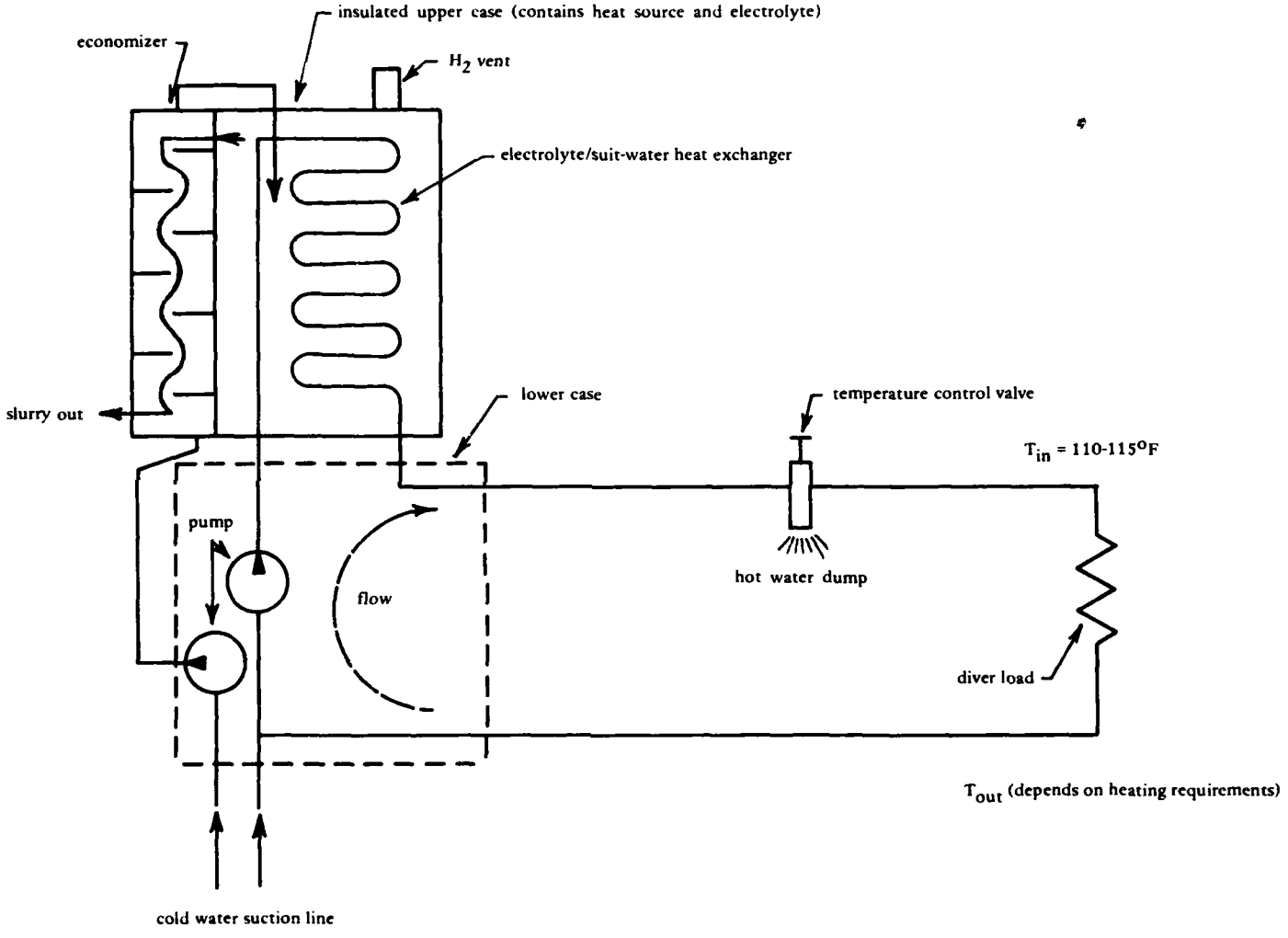

Figure 23. Schematic of 8-kW-hr experimental heater.

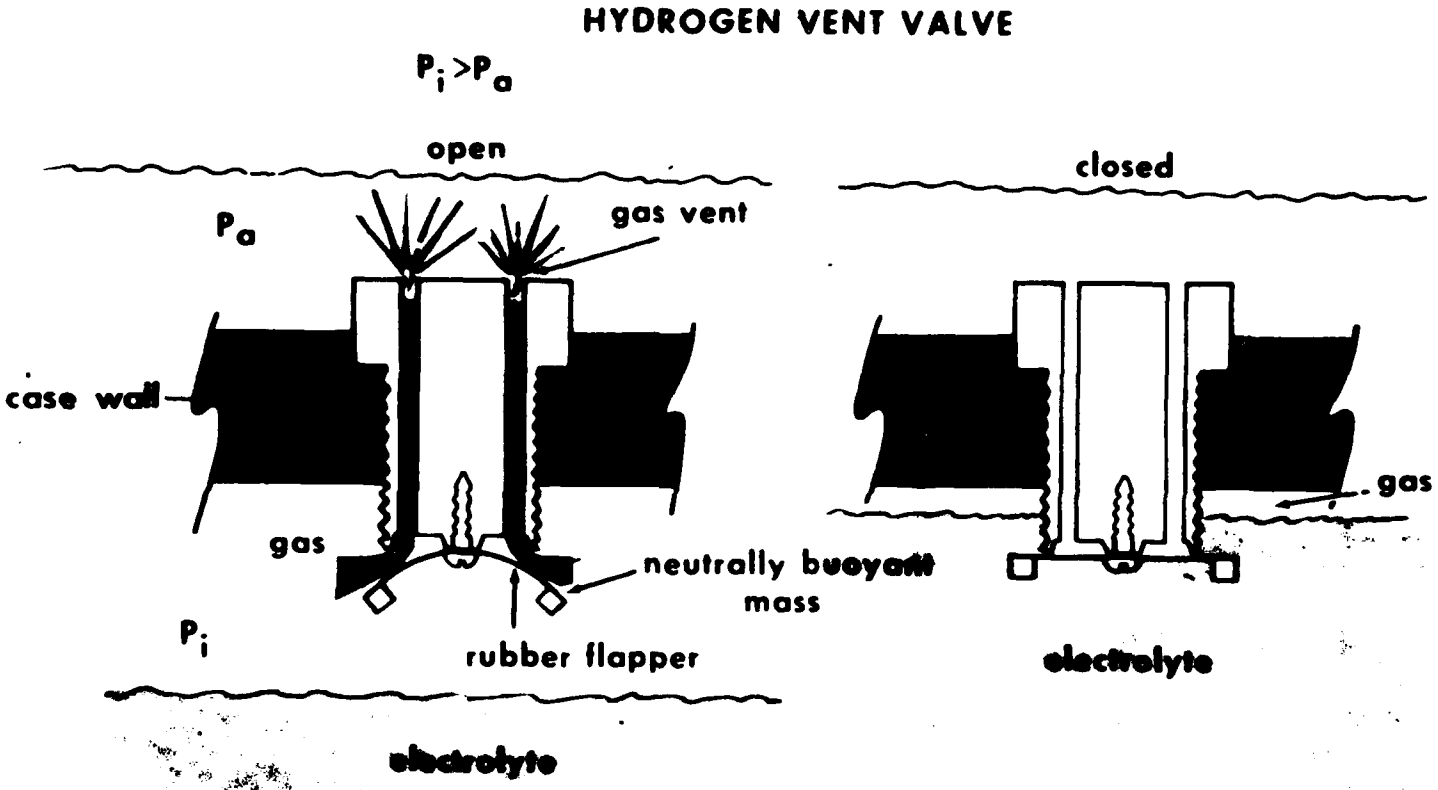

Figure 24. Schematic of hydrogen vent valve.

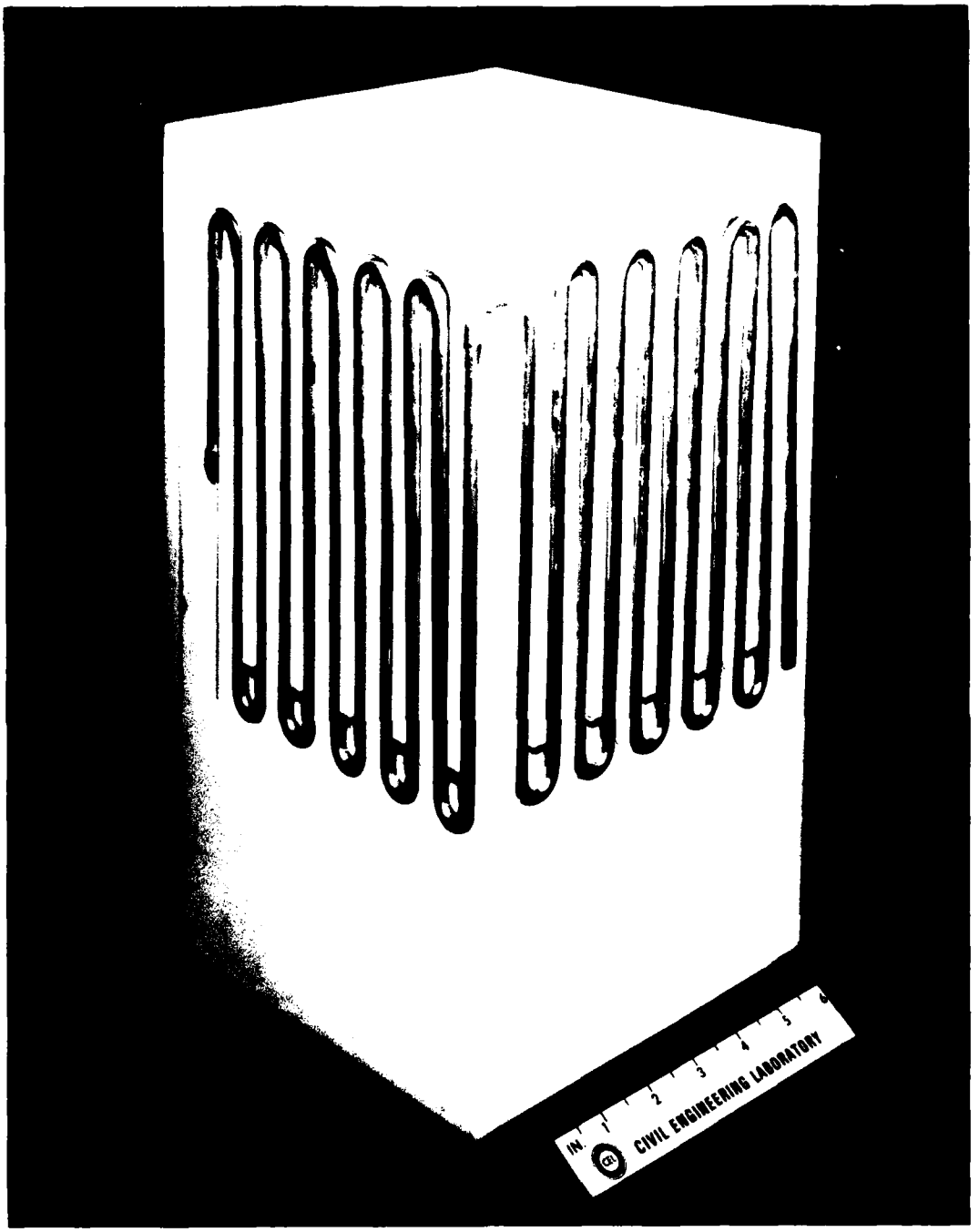

Figure 25. Economizer heat exchanger built into case of 8-kW-hr diver heater.

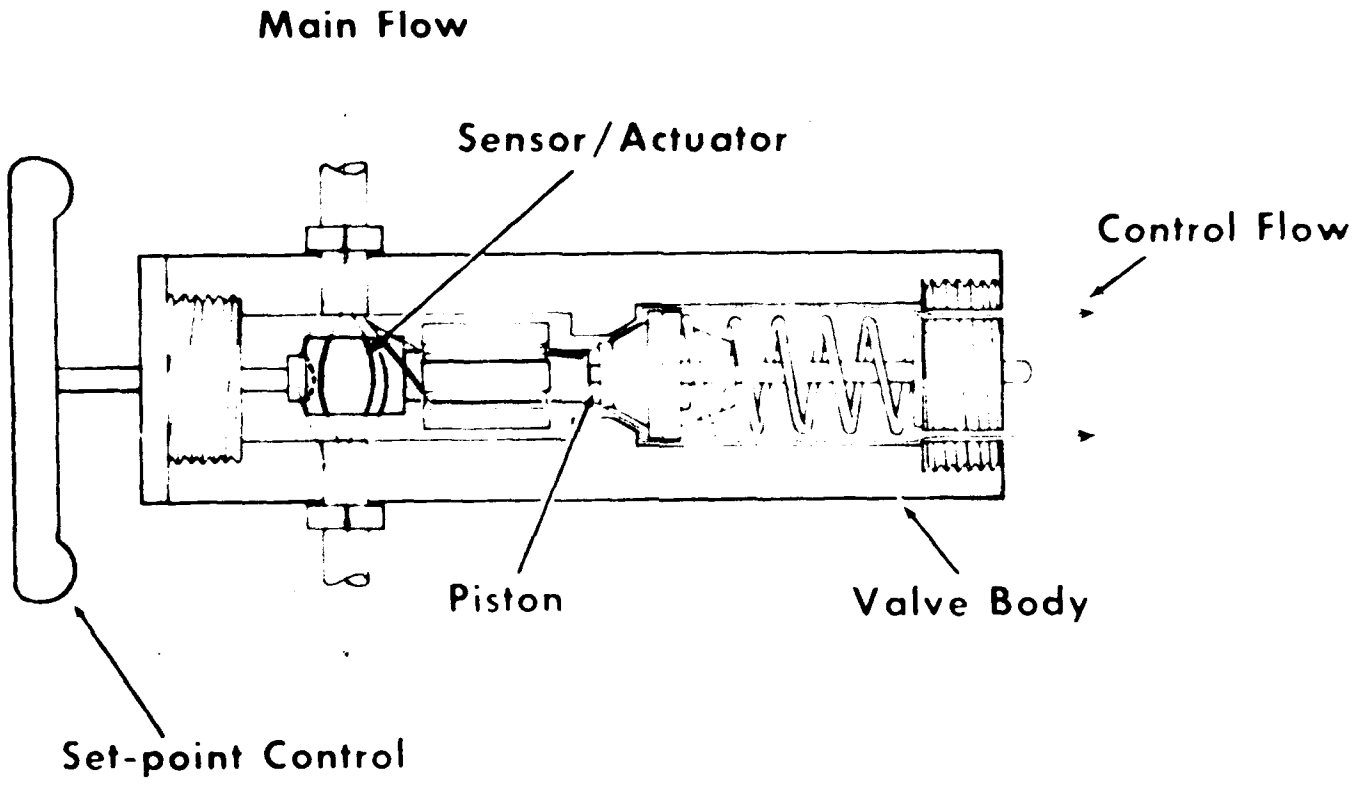

TEMPERATURE CONTROL VALVE

Figure 26. Schematic of temperature control valve.

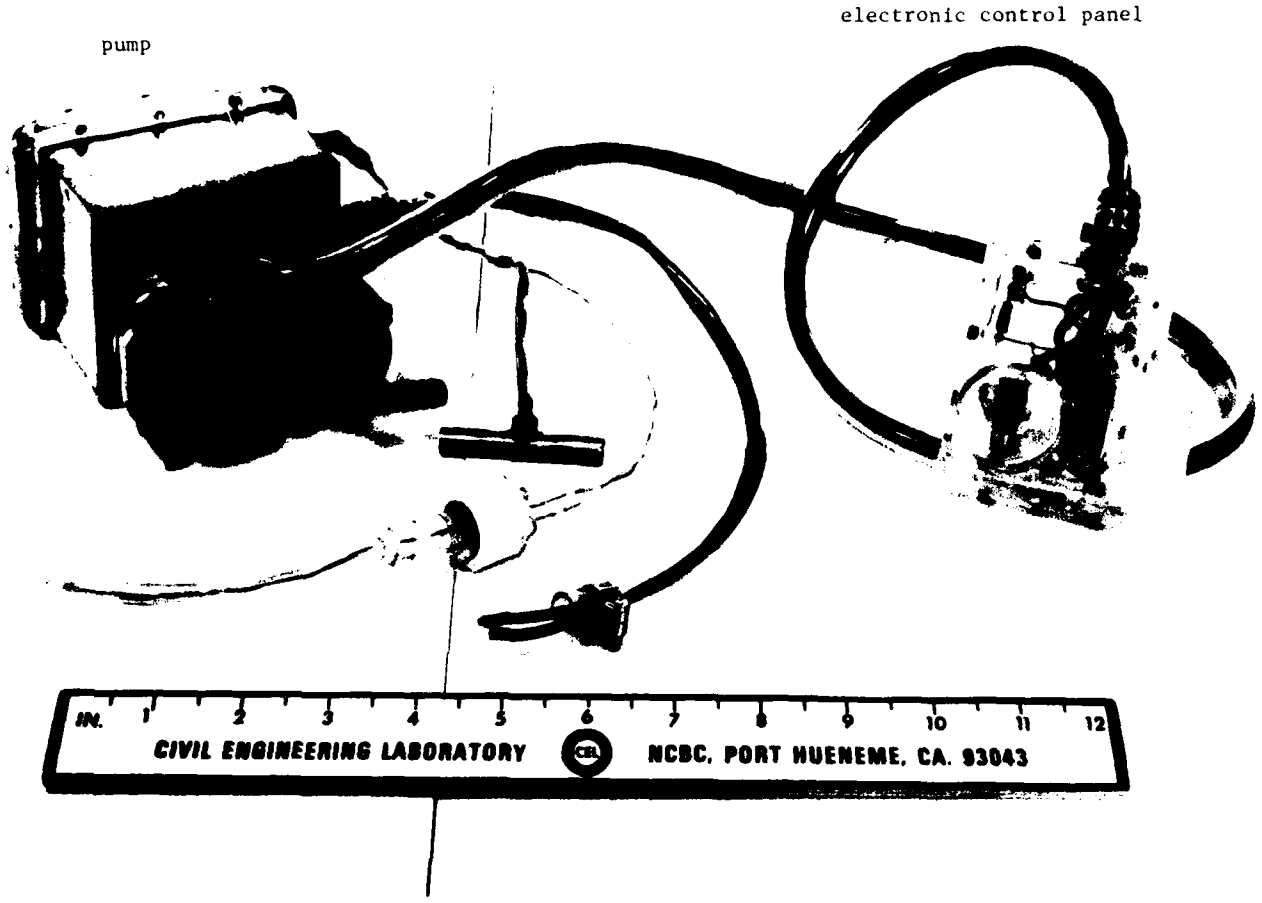

Figure 27. Diver suit water and fresh electrolyte pumps alloy with electronic control panel.

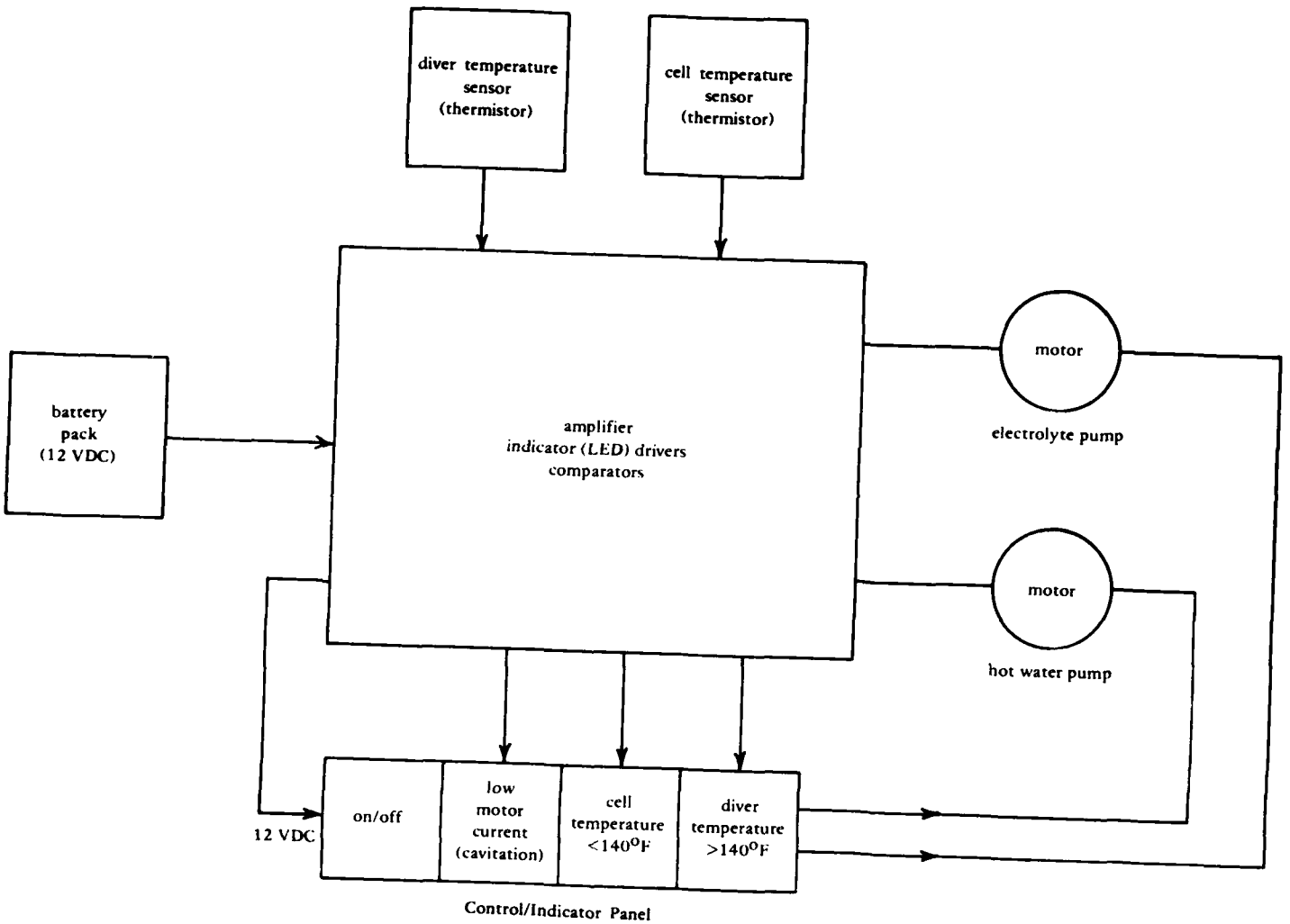

Figure 28. Electronic/circuit for pumps.

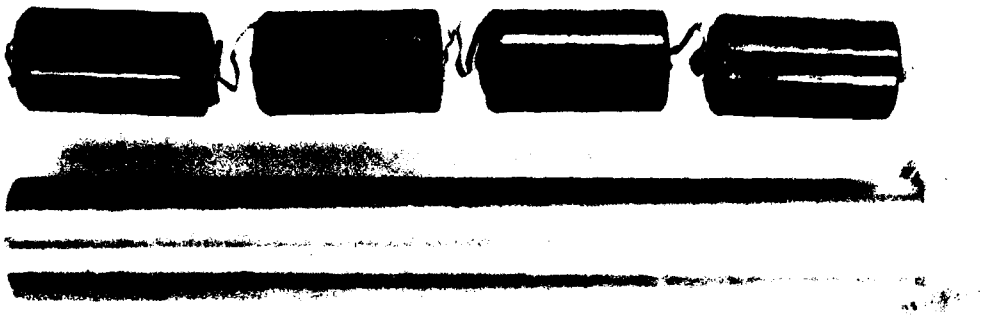

Figure 29. Battery case (one of three) and a set of lithium primary batteries.

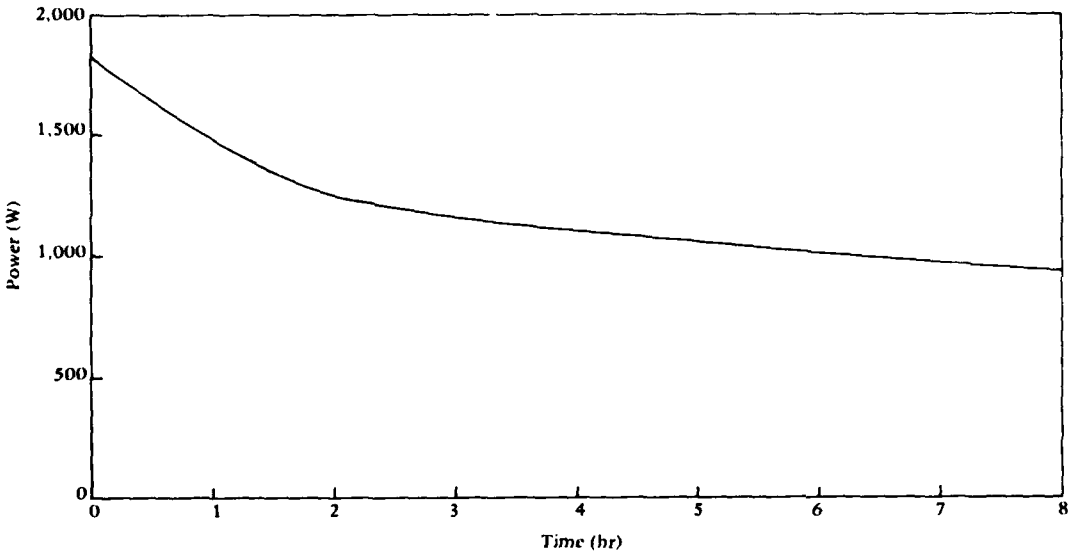

Figure 30. Power curve for 8-kW-hr heater tests.

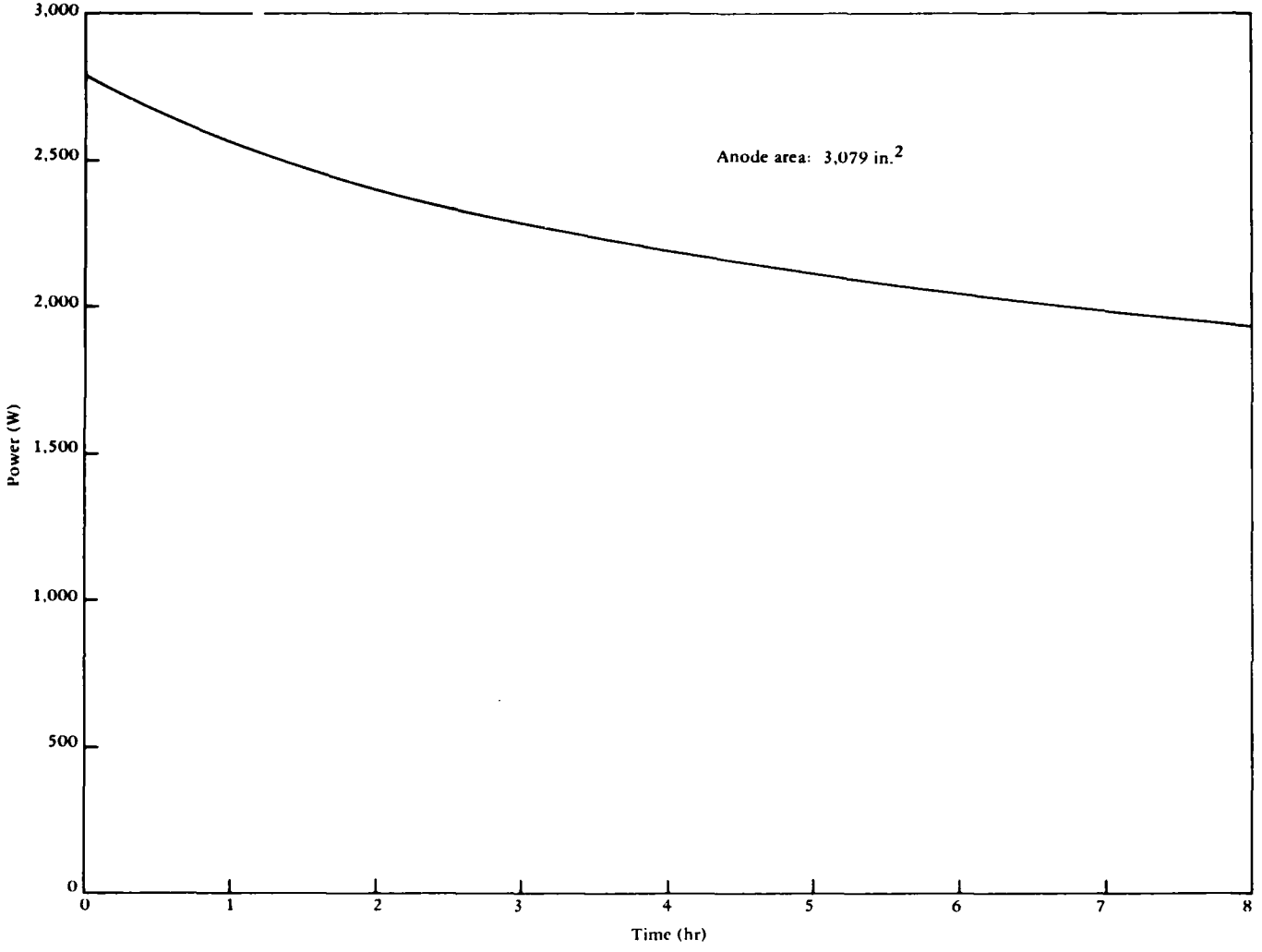

Figure 31. Power curve for 16-kW-hr heater tests.

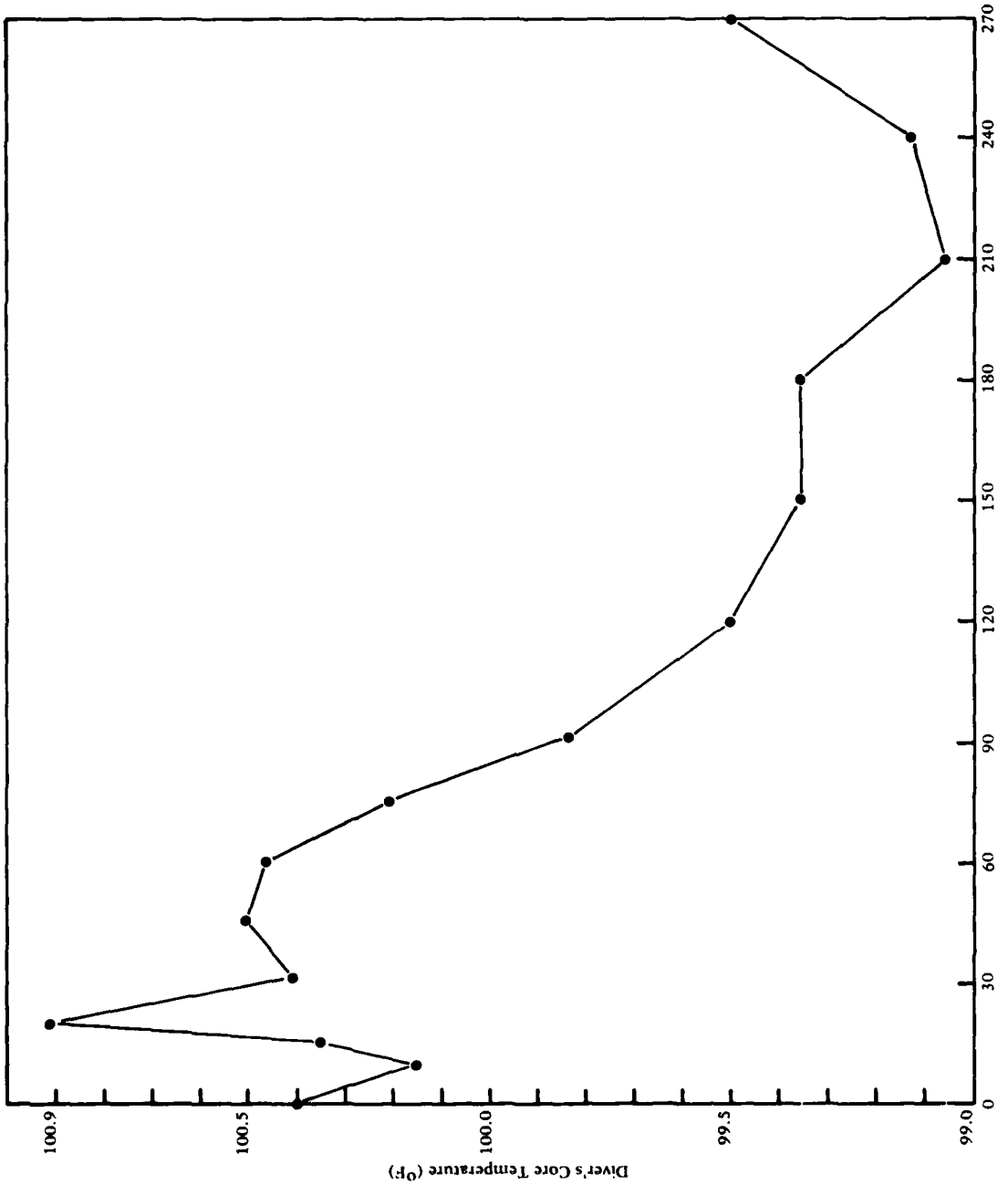

Figure 32. Diver's core temperature curve for heater tests.

Figure 33. Mock-up of chest-mounted diver heater under Mark 6 UBA breathing bag.

Table 1. Energy Values of Various Reactants

(e = electrical output, t = thermal output,
NEA = no experimental values available.)

Source	Energy Produced (W-hr/lb)	
	Theoretical	Actual
Batteries		
Proposed magnesium seawater reaction, $Mg + H_2O(Fe)$	1,850	$1,800_t$ 400_e
Magnesium-silver chloride (torpedo battery)	90	70_e
Lead-acid (secondary storage battery)	74	15_e
Silver oxide-zinc (silver cell)	201	50_e
Manganese dioxide-zinc (dry cell)	130	25_e
Nickel-cadmium	96	15_e
Mercury oxide-zinc (mercury cell)	104	40_e
Zinc-air (air batteries)	400	80_e
Sodium-oxygen (battery)	1,010	250_e
Magnesium bromide (experimental organic cathode)	250	60_e
Sodium sulfur (experimental)	350	150_e
Lithium chloride (experimental high-temperature-fused chloride)	1,000	250_e
Lithium fluoride (experimental)	750	100_e

continued

Table 1. Continued

(e = electrical output, t = thermal output,
NEA = no experimental values available.)

Source	Energy Produced (W-hr/lb)	
	Theoretical	Actual
Combustion		
Fuel oil and liquid oxygen	1,370	$1,370_t$
Fuel oil and 90% hydrogen peroxide	970	970_t
Butane-O_2		$2,100_t$
Latent Heat		
Lithium hydride (sensible heat and change of state)	250	NEA
Lithium fluoride (sensible heat and change of state)	305	NEA
Boron (sensible heat)	290	NEA
Mono Fuel		
Hydrazine hydrate (decomposition)	1,520	NEA
Isotope		
Plutonium 238 (8-hour exposure)	---	200_t[a]

[a]Value includes weight of shielding and hardware.

Note: 1 W-hr/lb = 0.45 J/kg.

Table 2. Summary of Reaction Parameters and Their Effects

Parameter	Influence	Effect on the Reaction
Electrode gap	Cell internal resistance Free transport of reaction products	Decreasing gap increases reaction rate. Small gap can cause the products to clog the gap which excludes the electrolyte from anode surface, thus reducing the reaction rate.
Electrolyte temperature	Transport of ions; solubility of products	Raising temperature increases reaction rate; no noticeable effect on energy density.
Electrolyte pH	Rate of precipitation of $Mg(OH)_2$ near the anode	High pH can cause an $Mg(OH)_2$ barrier to form near anode, which excludes the electrolyte, thus reducing the reaction rate.
	Evolution of H_2 at the cathode	Low pH (excess H^+ ions) promotes the formation of H_2 at the cathode, increasing the reaction rate.
Electrolyte density	Transport of reaction products	An electrolyte thickened with reaction products slows the transport of fresh electrolyte to the electrodes, thus reducing the reaction rate. Also reduces removal of products and increases pH at anode.

continued

Table 2. Continued

Parameter	Influence	Effect on the Reaction
Hydrogen gas volume in electrolyte	Cell internal resistance; electrolyte circulation	Gas bubbles displace electrolyte from contact with the anode, reducing reaction rate. (The effect of the gas is particularly evident near the top of the cell where there is the largest proportion of gas bubbles. After the anodes have reacted for some time, they are tapered, with the thickest portion being at the top.)
Anode composition	Reaction product consistency	Pure magnesium produces a fluffy product that easily clogs the electrode gap (decreases reaction rate). AZ-31B-O or AZ-31B-H24 magnesium alloy produces a product that readily precipitates (does not slow reaction rate except after much precipitation has accumulated). Other anode compositions have been investigated, but AZ31B was selected on the basis of availability, performance, low cost, and lack of pollutants, such as Hg.
Cathode composition	Unknown	Iron cathodes produce a reasonable reaction rate; other cathodes produce significantly lower rates.

continued

Table 2. Continued

Parameter	Influence	Effect on the Reaction
	Internal cell resistance	An iron-plated copper cathode exhibits an accelerated reaction rate, probably due to the decreased resistance of the copper substrate.
Anode physical condition	——	The area of the anode exposed to the electrolyte determines the reaction rate: more area - greater rate.
Cathode physical condition	Polarization (hydrogen overvoltage)	Rough surface cathode produces a higher reaction rate than a smooth cathode.
Electrolyte composition	Internal cell resistance; ion mobility	High salinity produces high reaction rates.

Table 3. Tests to Accelerate and Slow Reaction Rate

Test	Function	Description	Results
Electrolyte dilution	Slow initial reaction rate	Mix freshwater with initial charge of seawater electrolyte to retard initial reaction; mixing by adding makeup electrolyte; the cell output returns to normal as ion concentration increases	As shown in Figure 12, diluted seawater reduces reaction rate; thus, energy can be conserved during first hours of operation. 30% seawater reduces rate to approximately 50%
Coat anode surface	Slow initial reaction rate	Coat anode surface with a number of materials; as reaction proceeds, coating would be removed, and reaction rate would return to normal	
		Spray lacquer, silicone rubber, silicone vacuum grease, gasket compound	Remained on plates too long, thus would not permit reaction to proceed at usable rate

continued

Table 3. Continued

Test	Function	Description	Results
		Spray vinyl	Came off in sheets, which could clog pumps and block electrolyte passage between plates
		Rust inhibitor, automotive grease, automobile wax	Reaction removed contaminant too rapidly from plates
		Chemical treatment of anodes, chrome pickle, dilute chromic	No noticeable effect
		Insulating spray paint	Spalled from anode within 1 hour; worked reasonably well; particles remained in electrolyte, causing potential clogging
Reduce cathode thickness	Slow reaction rate	Use a thin cathode that would limit current-carrying capability during initial high reaction rate and function normally at later hours of test	Figure 10 shows that cathode thickness can limit reaction rate

continued

Table 3. Continued

Test	Function	Description	Results
Reduce anode edge effect	Slow initial reaction rate	Fabricate cathodes smaller than anodes so that distance from cathode to anode edges is greater than plate spacing, thus slowing edge reaction; cathodes fabricated so that edge was about 1/8 in. laterally from anode edge	Small-scale tests indicated that edge effect was reduced
Sheared versus sawed anodes	Increase life of anode edge	Fabricate anodes with machined edges and compare them to sheared edges. Anodes in past have been cut by shearing. This leaves edges of anode irregular with high stress areas and fragments. The result is a larger effective anode area on edge	Plates seemed to hold dimensions longer with machined edges; more stable reaction rate

continued

Table 3. Continued

Test	Function	Description	Results
Reduce anode edge effect	Increase life of anode edge	Apply different coatings to anode edges	Silicon rubber seemed to be effective at reducing edge effect
Saturated salt in seawater	Accelerate reaction rate	Prepare saturated solutions of seawater and salt; sample cells were run in solution	Power densities 1.5 to 3 times greater than normal were obtained; however, sludge would not settle, and reaction rate decayed because of clogging
Increasing driving potential	Accelerate reaction rate	Increase reaction rate by increasing driving potential using plated cathodes; nickel, silver, and gold plating tested	None of the materials provided improvement over iron cathodes
Substitute cathodes	Accelerate reaction rate	Fill voids in iron screen cathode with inert material; reduce polarization	Significantly lower reaction rate
Substitute cathode	Accelerate reaction rate and reduce hydrogen	Use MnO_2 cathode on iron screen to produce an active cathode	Cathode clogged with $Mg(OH)_2$ and reaction decayed; both O_2 and H_2 produced

continued

Table 3. Continued

Test	Function	Description	Results
Anode thickness	Increase reaction rate during final hours	Test several thin anodes in Dewar to compare with standard cell	No significant change in reaction rate

Table 4. Comparison of Reaction Control Methods

Type of Control Attempted	Expected Effect	Mechanism	Results
pH	Reduce high pH which causes surface blocking of reaction at anode	Controlled addition of fresh seawater	Large volumes required to make significant changes; results in excessive losses from preheating seawater
		Chemical additives	Required excessive amounts; also most additives caused reaction changes that resulted in initially high reaction rates and then markedly reduced rates a short time later
Variable Plate Spacing	Decreasing gap results in increasing reaction rate	Mechanically drive plates together, e.g., electric motors or manual screw	Works, but requires excessive weight and volume; automatic feature is complicated
Constant Plate Spacing	Maintain constant gap; constant reaction rate	Provide spacer between plates while self-adjusting anode is consumed	A number of apparatus tried; most unique and effective is shown in Figure 13; cone is inert, chamfer angle and cone angle determine movement. Small-scale test was successfully run; a simplified arrangement is yet to be developed. Providing short circuit is a problem

continued

Table 4. Continued

Type of Control Attempted	Expected Effect	Mechanism	Results
Variable Resistance	Limit current flow between anode and cathode	Variable resistance in place of short circuit	Resistance has to be variable in the range of 0 to 10^{-3} ohms between each plate; not practical
Variable Anode Area	Adjust anode area, thus increasing or decreasing reaction rate	Separate plate stacks — one of iron, one of magnesium — move so that anode area increases or decreases	Works, but requires excessive volume to accommodate adequate power change; approximately 50% greater in weight than fixed-plate cell

Table 5. Efficiency of Various Cathode Materials

Cathode Material	Percent By Weight	77°F Electrolyte			140°F Electrolyte		
		Initial Reaction Rate[a]	Steady Reaction Rate[b]	Percent Completion[c]	Initial Reaction Rate	Steady Reactio Rate	Percent Completion
Copper	10	16.0	4.0	49.5	14.2	4.4	45.0
Iron	10	7.6	2.8	32.4	7.6	2.2	32.4
Iron + Manganese dioxide	10 ea	6.8	3.0	36.0	8.0	2.8	28.8
Iron	50	6.6	1.8	20.5	2.0	1.0	11.0
Nickel	10	6.0	2.6	32.4	7.6	2.8	38.7
Platinum	10	4.8	2.2	28.8	9.0	3.0	34.2
Silver	10	2.0	1.5	21.6	1.0	4.8	40.4
Manganese	10	1.6	2.4	30.6	6.4	2.4	33.3
Graphite	10	1.4	1.4	21.6	5.4	1.8	21.6
Aluminum	10	1.2	0.6	6.3	1.0	1.0	18.0
None	—	1.0	0.8	14.2	3.0	0.8	11.0
Silicon	10	0.4	1.0	17.1	4.0	1.8	21.6
Manganese dioxide	10	0.6	1.2	9.0	3.0	1.2	18.0

[a] In ml of gas per gram of mixture per minute in the first 10 minutes of reaction.

[b] In ml of gas per gram of mixture per minute between 20 and 120 minutes of reaction time.

[c] Comparison between the actual amount of gas liberated in 4 hours and the amount of gas theoretically liberated in complete reaction of the same weight of pure magnesium.

Table 6. Cell Characteristics

Cell Type	Specific Output		Reaction Output Efficiency $\left(\frac{\text{Actual Energy}}{\text{Theoretical Energy}}\right)$	Relative Reactivity[a]	Relative Cost	Features
	Based on Mass	Based on Volume				
Dual plate	800 W-hr per pound of cell (6.4 MJ per kg)	36 W-hr per $in.^3$ of cell (8 kJ per cm^3)	0.8	1	1	1. Cell materials readily available 2. Low cost
Bi-polar	850 W-hr per pound of cell (6.8 MJ per kg)	36 W-hr per $in.^3$ of cell (8 kJ per cm^3)	0.85	1.2	1.5	1. Materials must be pre-processed 2. High efficiency 3. Separate iron plates not required
Powdered metal alloy	800 to 900 W-hr per pound of cell (6.4 to 7.1 MJ per kg)	46 to 52 W-hr per $in.^3$ of cell (10 to 11 kJ per cm^3)	0.9 to 0.95	1.6	1.5	1. Materials must be pre-processed 2. Very high efficiency 3. High reactivity 4. Variable power possible 5. Can be formed into plates

[a] Reactivity = watts per gram in the particular cell configuration.

APPENDIX

Human Factors Considerations in Self-Contained Diver Heater Design

by F. B. Barrett

BACKGROUND

A limited human factors analysis of self-contained diver heating systems was conducted to determine man/equipment interface requirements. The analysis was accomplished primarily through in-water test trials of several heater mock-ups and through discussions with combat swimmer personnel and appropriate Navy diving authorities. Equipment compatibility tests were also conducted during Swimmer Delivery Vehicle (SDV) operations by personnel using Navy Mark 6 underwater breathing apparatus.

PRELIMINARY CONSIDERATIONS

An analysis of underwater breathing apparatus (UBA) currently in use by Navy tactical swimmers and probable future configurations was conducted to determine possible locations for diver heater components. The major requirement placed on the analysis was to minimize the restrictions imposed on the swimmer and his mobility. As a result of this analysis, three heater mock-ups were fabricated for in-water test and evaluation (Figures 33, 34, and 35). A brief description of the mock-ups is contained in Table 7. All of the mock-ups were fabricated from wood and weighted for neutral buoyancy; the leading edges were faired to reduce hydrodynamic drag. The chest and wing tank mock-ups were configured to be compatible with the presently used Mark 6 UBA. The chest unit appeared to be compatible with all known types of Navy UBA's. Some UBA's have enclosed back packs that make adaptation of the back pack wing tank units very difficult.

A mock-up of the heater control panel was fabricated and is shown in Figure 36. The basic unit was 2 x 3 x 4 inches (5 x 8 x 10 cm). The control handle was 2 inches in diameter with pronounced knobs. Small diameter LEDs were simulated.

TESTS

The chest and wing tank mock-ups were tested in a swimming pool in conjunction with the Mark 6 UBA. The apparatus shown in Figure 37 was used to determine the mock-up drag characteristics. Divers were pulled through the water at 1-knot speeds while submerged. Considerable variability in the results was noted; however, the drag was verified as being a fraction of 1 pound.

Two divers swam laps in the swimming pool while submerged. They were asked to swim at a pace which they could maintain for long-duration swims. The objective of the test was to obtain their subjective feelings of heater interference with surface and underwater swimming. The results of the swimming test are contained in Table 8. Speed loss was judged to be noticeable, but not excessive. The divers indicated a preference for the chest mock-ups although, subjectively, neither mock-up seemed to interfere with their mobility. They felt that in the chest mode they could retain the diver heater unit in emergencies.

The mock-ups were further tested in conjunction with routine SDV-type operations. Combat-type divers were required to swim approximately one-half mile underwater and 100 yards on the surface using the back pack and chest mock-up heaters. The test results were in the form of subjective comparison by the divers. Interference with SDV operations was noted. Also, the divers stated that they would prefer having the heater mounted directly on a SDV in order to lessen the gear they have to carry.

RESULTS

1. Noticeable, but not excessive drag, was observed from swimming with the mock-ups.

2. Divers preferred the chest mock-ups, because it would be possible to retain the diver heater following ditching of the UBA.

3. Interference with swimming or arm movements with either of the mock-ups did not appear excessive.

4. Both mock-ups interferred with SDV-type operations.

   a. The chest unit resulted in difficulty in bending forward while seated, thus interferring with instrument reading.

   b. Divers could not bend far enough forward wearing the chest unit to open the flood doors of the SDV.

   c. While using the back pack mock-up, it was difficult to reach the Navy Mark 6 UBA bypass valve and air ON-OFF switch.

5. Divers reported no difficulty in reading the displays. It was quite simple to operate the controls using thin neoprene gloves; however, problems could be anticipated using three-fingered mittens.

CONCLUSIONS

1. Additional human-factors-type analyses are required to provide heater systems that will be compatible with both swimmer and SDV-type operations.

2. Most divers would prefer having an SDV-mounted heater to lessen gear requirements. This comment does not take into consideration the physiological requirements of operations in 28°F (-2°C) water. [Many divers appear to be unaware of the actual problems that result from extended operations in 28° to 30°F (-2 to -1°C) water.]

3. For diver-heating equipment to be acceptable to fleet units, it must be as compact, serviceable, and maintenance-free as possible.

4. Future heater units should be tested in conjunction with newer SDV's currently under development.

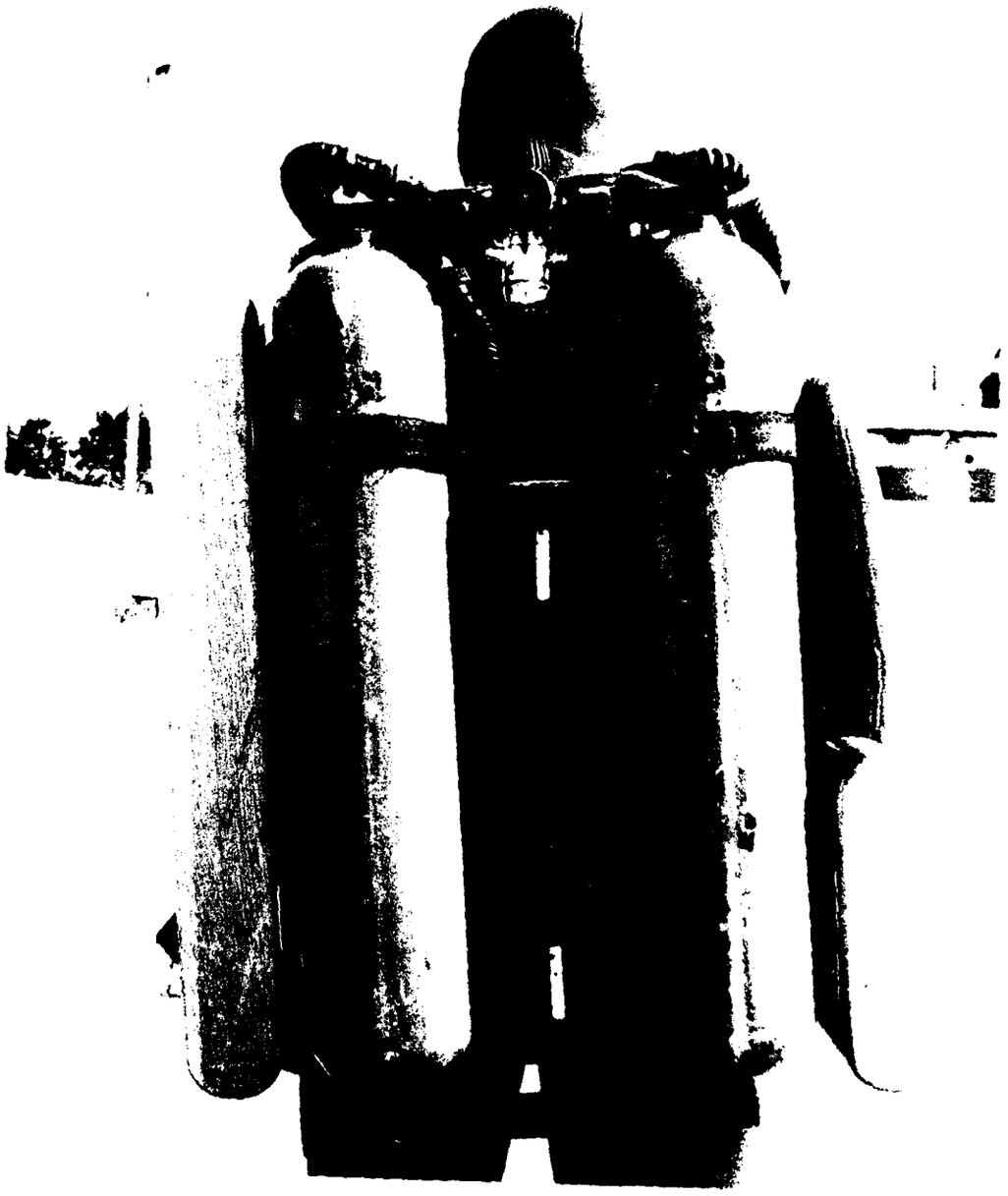

Figure 34. Mock-up of wing-tank-mounted diver heater.

Figure 35. Mock-up of backpack-mounted diver heater.

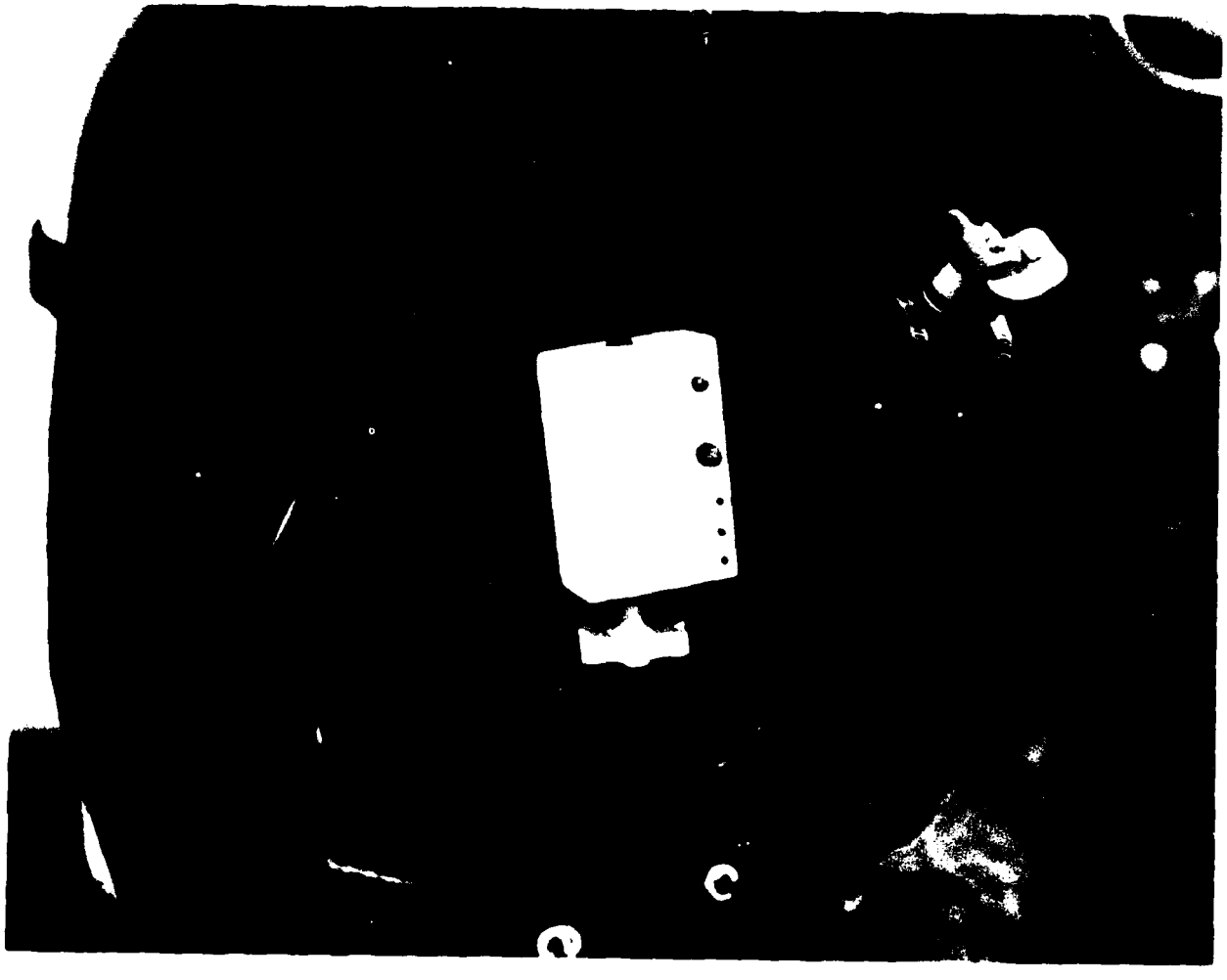

Figure 37. Mock-up of heater control panel.

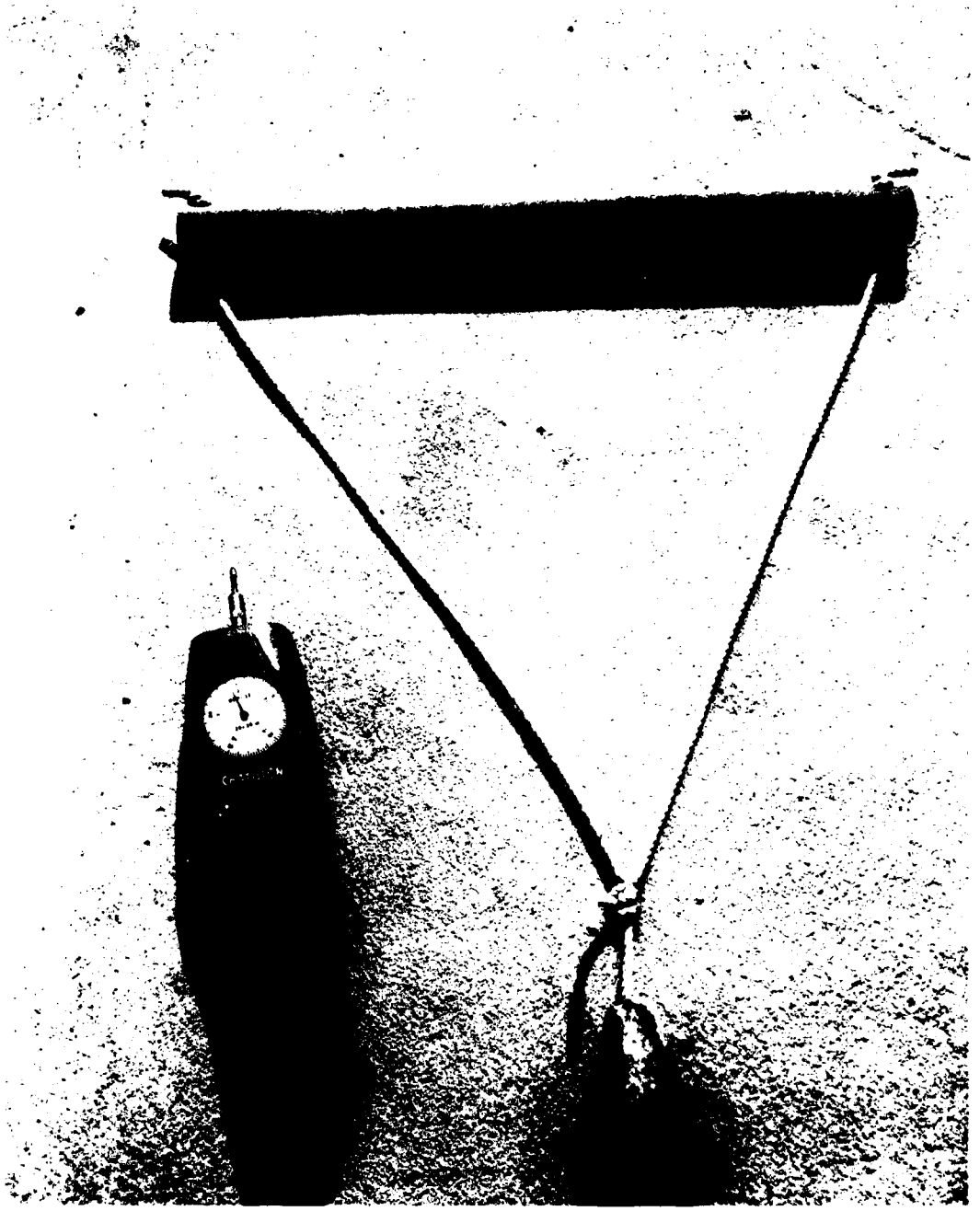

Figure 37. Diver drag test apparatus.

Table 7. Description of Mocks-ups

Mock-Up Type	Description	Predicted Capacities
Chest	3 in. thick x 12 in. wide x 14 in. long; worn under breathing bag	8 kW-hr 2 kW for 4 hr
Wing tanks	2 in. x 3-1/2 in. x 25 in., plus 2 in. x 3-1/2 in. x 10 in; attaches to outer sides of gas tanks	4 kW-hr 1 kW for 4 hr
Backpack	4-1/8 in. x 6-1/4 in. x 24 in.; attaches to back of breathing gas tanks	8 kW-hr 2 kW for 4 hr

Note: 1 in. = 2.54 cm.

Table 8. Mock-up Performance Tests in Swimming Pool

Diver Gear	Speed (mph) for —		Mean Speed Loss (mph)
	Diver A	Diver B	
Mark 6 UBA	1.12	1.48	-
Mark 6 UBA plus chest heater unit	1.08	1.51	0.015
Mark 6 UBA plus wing tank heater unit	1.06	1.37	0.075

Note: 1 mph = 1.6 km/hr.

DISTRIBUTION LIST

AF ENVIRON. HEALTH LAB McClellan AFB CA
AFB (AFIT/LD), Wright-Patterson OH; ABG/DEE (F. Nethers), Goodfellow AFB TX; CESCH, Wright-Patterson; SAMSO/DEB, Norton AFB CA; Stinfo Library, Offutt NE
ARMY AMSEL-GG-TD, Fort Monmouth NJ; BMDSC-RE (H. McClellan) Huntsville AL; DAEN-CWE-M (LTC D Binning), Washington DC; DAEN-FEU, Washington DC; DAEN-MCE-D Washington DC; Natick Laboratories (Kwoh Hu) Natick MA; Tech. Ref. Div., Fort Huachuca, AZ
ARMY BALLISTIC RSCH LABS AMXBR-XA-LB, Aberdeen Proving Ground MD
ARMY COASTAL ENGR RSCH CEN Fort Belvoir VA
ARMY CONSTR ENGR RSCH LAB Library, Champaign IL
ARMY CORPS OF ENGINEERS Seattle Dist. Library, Seattle WA
ARMY CRREL A. Kovacs, Hanover NH
ARMY DEV READINESS COM AMCPM-CS (J. Carr), Alexandria VA
ARMY ENG WATERWAYS EXP STA Library, Vicksburg MS
ARMY ENGR DIST, Library, Portland OR
ARMY MISSILE COMMAND Redstone Sci. Info. Center (Documents), Redstone Arsenal AL
ARMY MOBIL EQUIP R&D COM Mr. Cevasco, Fort Belvoir MD
ASST SECRETARY OF THE NAVY Spec. Assist Energy (P. Waterman), Washington DC; Spec. Assist Submarines, Washington DC
BUREAU OF RECLAMATION Code 1512 (C. Selander) Denver CO
MCB ENS S.D. Keisling, Quantico VA
CNAVRES Capt J. A. Erickson, New Orleans LA
CNM Code 03Z
CNO Code OPNAV 96H; OP987P4 (B. Petrie), Pentagon
COMCBPAC Operations Off, Makalapa HI
COMNAVMARIANAS Code N4, Guam; FCE, Guam
COMSUBDEVGRUONE Operations Offr, San Diego, CA
COMTWELFTHNAVDIST San Francisco CA
DEFENSE DOCUMENTATION CTR Alexandria, VA
DTNSRDC Code 1548 (T. Tsai), Bethesda MD
DTNSRDC Code 522 (Library), Annapolis MD
ENERGY R&D ADMIN, Dr. Vanderryn, Washington DC; INEL Tech. Lib. (Reports Section), Idaho Falls ID
ENVIRONMENTAL PROTECTION AGENCY MD-18(P. Halpin), Research Triangle Park NC; Reg. VIII, 8M-ASL, Denver CO
FLTCOMBATDIRSYSTRACENLANT PWO, Virginia Bch VA
GSA Office of Const. Mgmt (M. Whitley), Washington DC
HQFORTRPS 2nd FSCG, (Caudillo) Camp Lejeune, NC
KWAJALEIN MISRAN BMDSC-RKL-C
MARINE CORPS BASE Maint. Office, Camp Pendleton CA
MARINE CORPS HQS Code LFF-2, Washington DC
MCAS Code S4, Quantica VA
MCB Base Maint. Offr, Quantico VA
MCRD PWO, San Diego Ca
NAD Code 011B-1, Hawthorne NV
NAS Asst C/S CE; Lead, Chief, Petty Offr PW/Self Help Div, Beeville TX; PWO, Millington TN; ROICC Off (J. Sheppard), Point Mugu CA; SCE Lant Fleet
NAVSHIPYD Commander, Vallejo, CA
NAVCOASTSYSLAB Code 710 (R. Elliott), Code 710.5 (J. Mittleman); Code 710.5 (J. Quirk); Library
NAVCOMMSTA PWO, Fort Amador Canal Zone
NAVFACENGCOM Code 0433B, Code 0451, Code 04B5, Code 081B; Code 101; Code 102 (CDR Dettbarn), Code 1023 (M. Carr); PC-22 (F. Spencer), PL-2
NAVHOSP LTR, Elsbernd, Puerto Rico
NAVOCEANO Code 1600; Code 3412 (J. Kravitz)
NAVORDSTA PWO, Louisville KY
NAVPGSCOL E. Thornton, Monterey CA
NAVPHIBASE Code S3L, Norfolk VA; OIC, UCT-1

NAVREGMEDCEN SCE (LCDR B. F. Thurston), San Diego CA
NAVSCOLCECOFF C35
NAVSECGRUACT PWO, Torri Sta, Okinawa
NAVSHIPYD Code 400, Puget Sound; Code 410, Mare Is., Vallejo CA; Code 440, Norfolk; SCE, Pearl Harbor HI
NAVSTA CO, PWD (L. Ross), Midway Island
NAVSUPPACT CO, Seattle WA; Code 4, 12 Marine Corps Dist, Treasure Is., San Francisco CA
NATL RESEARCH COUNCIL Naval Studies Board, Washington DC
NAVAIRSYSCOM L.T.W. Hall, Washington DC
NAVAL FACILITY PWO, Cape Hatteras, Buxton NC; PWO, Centerville Bch, Ferndale CA
NAVCONSTRACEN CO (CDR C.L. Neugent), Port Hueneme, CA
NAVEODFAC Code 605, Indian Head MD
NAVFACENGCOM CDR L.K Donovan, Alexandria VA; Code 0453 (D. Potter); Code 1023 (T. D. Stevens), Alexandria VA
NAVFACENGCOM - CHES DIV, Code 403 (H. DeVoe); Code FPO-1 (C. Bodey), Code FPO-1 (Ottsen); Code FPO-1C2; Code FPO-1SP13 (T.F Sullifan)
NAVFACENGCOM - LANT DIV, RDT&ELO 09P2, Norfolk VA
NAVFACENGCOM - NORTH DIV, Code 1028, RDT&ELO, Philadelphia PA; ROICC, Contracts, Crane IN
NAVFACENGCOM - PAC DIV, Code 402, RDT&E, Pearl Harbor HI; Commanders
NAVFACENGCOM - SOUTH DIV, Code 90, RDT&ELO, Charleston SC; Dir., New Orleans LA
NAVFACENGCOM - WEST DIV, 112; AROICC, Contracts, Twentynine Palms CA; Codes 09PA; 09P 20
NAVFACENGCOM CONTRACTS Bethesda, Design Div. (R. Lowe) Alexandria VA; Eng Div dir, Southwest Pac, PI, ROICC (LCDR J.G. Leech), Subic Bay, R.P.; ROICC, Pacific, San Bruno CA; TRIDENT (CDR J.R. Jacobsen), Bremerton WA 98310
NAVMARCORESTRANCEN ORU 1118 (Cdr D.R. Lawson), Denver CO
NAVNUPWRU MUSE DET OIC, Port Hueneme CA
NAVPETOFF Code 30, Alexandria VA
NAVPETRES Director, Washington DC
NAVPGSCOL Code 2124 (Library), Monterey CA
NAVSEASYSCOM Code SEA OOC
NAVSECGRUACT PWO, Edzell Scotland
NAVSHIPYD Code 202.4, Long Beach CA; Code 202.5 (Library) Puget Sound, Bremerton WA; Code Portsmouth NH, Library, Portsmouth NH
NAVSUPPACT AROICC (LT R.G. Hocker), Naples Italy
NAVWPNSUPPCEN PWO
NAS Code 18E (ENS P.J. Hickey), Corpus Christi TX; OIC, CBU 417, Oak Harbor WA; PWD (ENS F.S. Agonoy), Chase Field, Beeville TX; PWD (M.B. Trewitt), Dallas TX
NATL OCEAN AND ATMDS. ADMIN. Libraries Div.-D823, Silver Spring MD
NAVCOASTSYSLAB CO, Panama City FL
NAVCOMMSTA PWO, Norfolk VA
NAVELEXSYSCOM Code PME-124-61, Washington DC
NAVFACENGCOM - WEST DIV, Code 04B
NAVFACENGCOM CONTRACTS Code 09E, TRIDENT, Bremerton WA
NAVOCEANSYSCEN CODE 4099 (E. Hamilton), San Diego CA; Code 409 (D. G. Moore), San Diego CA; Code 6344 (R. Jones); Code 65 (H. Talkington); Code 6565 (Tech. Lib.), San Diego CA; Code 6700; Research Lib., San Diego CA; SCE (Code 6600), San Diego CA
NAVPGSCOL D. Leipper, Monterey CA
NAVSEC Code 6034 (Library), Washington DC
NAVSHIPYD Code 453 (H. Clements), Vallejo CA; PWD (LT N.B. Hall), Long Beach CA
NAVTRAEQUIPCEN Technical Library, Orlando FL
NAVWPNSTA Code 092A (C. Fredericks) Seal Beach CA
NAVXDIVINGU LT A.M. Parisi, Panama City FL
PMTC Code 4253-3, Point Mugu CA
NCBC CEL (CAPT N. W. Petersen), Port Hueneme, CA; CEL AOIC; Code 10; PW Engrg, Gulfport MS
NCBU 411 OIC, Norfolk VA
NMCB 133 (ENS T.W. Nielsen); 5, Operations Dept.; One, LT E.P. Digeorge
NRL Code 8441 (R.A. Skop), Washington DC
NROTCU Univ Colorado (LT D R Burns), Boulder CO
NSC Code 703 (M. Miller), Pearl Harbor HI; F. Wynne, Norfolk VA

NTC Code 54 (ENS P. G. Jackel), Orlando FL; Commander
NUSC Code EA123 (R.S. Munn), New London CT; Code S332, B-80 (J. Wilcox); Code SB 331 (Brown), Newport RI; Code TA131 (G. De la Cruz), New London CT
OCEANAV Mangmt Info Div., Arlington VA
OCEANSYSLANT LT A.R. Giancola, Norfolk VA
ONR CDR Harlett, Boston MA
OFFICE SECRETARY OF DEFENSE OASD(I&L) Pentagon (T. Casberg), Washington DC
ONR Code 484, Arlington VA; Dr. A. Laufer, Pasadena CA
PACMISRANFAC CO, Kekaha HI
PMTC Pat. Counsel, Point Mugu CA
PWC Code 116 (ENS A. Eckhart); Code 120C (A. Adams); Code 505A (H. Wheeler); ENS J.A. Squatrito, San Francisco Bay, Oakland CA; OIC CBU-405, San Diego CA;
USCG (G-ECV/61) (Burkhart) Washington, DC; HQ (GECV-3), Washington DC; MMT-4, Washington DC
USCG ACADEMY LT N. Stramandi, New London CT
USCG R&D CENTER CO; D. Motherway, Groton CT; Tech. Dir.
USNA Ch. Mech. Engr. Dept; Energy-Environ Study Grp, Annapolis, MD; Engr. Div. (C. Wu) Annaplolis MD; Environ. Prot. R&D Prog. (J. Williams), Annapolis MD; Sys. Engr Dept (Dr. Monney), Annapolis MD; Sys. Engr. Dept (R. McCoy)
AMERICAN UNIVERSITY Washington DC (M. Norton)
ARIZONA State Energy Programs Off., Phoenix AZ
CALIFORNIA INSTITUTE OF TECHNOLOGY Pasadena CA (Keck Ref. Rm)
CALIFORNIA STATE UNIVERSITY LONG BEACH, CA (CHELAPATI); LONG BEACH, CA (YEN)
COLORADO STATE UNIV., FOOTHILL CAMPUS Engr Sci. Branch, Lib., Fort Collins CO
CORNELL UNIVERSITY Ithaca NY (Serials Dept, Engr Lib.)
DAMES & MOORE LIBRARY LOS ANGELES, CA
FLORIDA ATLANTIC UNIVERSITY BOCA RATON, FL (MC ALLISTER)
FLORIDA ATLANTIC UNIVERSITY Boca Raton FL (W. Tessin)
FLORIDA TECHNOLOGICAL UNIVERSITY ORLANDO, FL (HARTMAN)
FUEL & ENERGY OFFICE CHARLESTON, WV
GORDON MC KAY LIB Cambridge, MA (Tech Report Collection)
HAWAII STATE DEPT OF PLAN. & ECON DEV. Honolulu HI (Tech Info Ctr)
INDIANA ENERGY OFFICE Office of Petroleum Allocation, Indianapolis IN
IOWA STATE UNIVERSITY Ames IA (CE Dept, Handy)
VIRGINIA INST. OF MARINE SCI. Gloucester Point VA (Library)
LEHIGH UNIVERSITY BETHLEHEM, PA (MARINE GEOTECHNICAL LAB., RICHARDS); Bethlehem PA (Linderman Lib. No.30, Fleeksteiner)
LIBRARY OF CONGRESS WASHINGTON, DC (SCIENCES & TECH DIV)
LOUISIANA DIV NATURAL RESOURCES & ENERGY Dept. of Conservation, Baton Rouge LA
LOW COUNTRY REG. PLAN. COUNCIL YEMASSEE, SC (BAGGS)
MAINE MARITIME ACADEMY CASTINE, ME (LIBRARY)
MASSACHUSETTS INST. OF TECHNOLOGY Cambridge MA (Rm 10-500, Tech. Reports, Engr. Lib.); Cambridge MA (Rm 14 E210, Tech. Report Lib.)
MICHIGAN TECHNOLOGICAL UNIVERSITY HOUGHTON, MI (HAAS)
MISSOURI ENERGY AGENCY Jefferson City MO
MIT Cambridge, MA (Harleman)
NATL ACADEMY OF ENG. ALEXANDRIA, VA (SEARLE, JR.)
NY CITY COMMUNITY COLLEGE BROOKLYN, NY (LIBRARY)
OHIO STATE UNIVERSITY COLUMBUS, OH (INST. OF POLAR STUDIES)
OREGON STATE UNIVERSITY CORVALLIS, OR (CE DEPT, BELL); LT R.B. Steimer, NROTC Unit, Corvallis OR
PENNSYLVANIA STATE UNIVERSITY STATE COLLEGE, PA (SNYDER)
PURDUE UNIVERSITY LAFAYETTE, IN (ALTSCHAEFFL); LAFAYETTE, IN (CE LIB); Lafayette IN (Leonards)
SCRIPPS INSTITUTE OF OCEANOGRAPHY LA JOLLA, CA (ADAMS); San Diego, CA (Marina Phy. Lab. Spiess)
STANFORD UNIVERSITY STANFORD, CA (DOUGLAS)
STATE ENERGY OFF. ATLANTA, GA (BONHAM)
STATE HOUSE AUGUSTA, ME (MAINE STATE FUEL ALLOC & CONSERV. OFF.)
STATE UNIV. OF NEW YORK FORT SCHUYLER, NY (LONGOBARDI)

TEXAS A&M UNIVERSITY COLLEGE STATION, TX (CE DEPT); College TX (CE Dept, Herbich)
BONNEVILLE POWER ADMIN Los Angeles CA (Hancock Lib. of Bio. & Ocean)
UNIVERSITY OF CALIFORNIA BERKELEY, CA (CE DEPT, GERWICK); BERKELEY, CA (CE DEPT, MITCHELL); BERKELEY, CA (OFF. BUS. AND FINANCE, SAUNDERS); Berkeley CA (E. Pearson); DAVIS, CA (CE DEPT, TAYLOR); La Jolla CA (Acq. Dept, Lib. C-075A); SAN DIEGO, CA, LA JOLLA, CA (SEROCKI)
UNIVERSITY OF DELAWARE Newark, DE (Dept of Civil Engineering, Chesson)
UNIVERSITY OF HAWAII HONOLULU, HI (CE DEPT, GRACE); HONOLULU, HI (SCIENCE AND TECH. DIV.)
UNIVERSITY OF ILLINOIS URBANA, IL (DAVISSON); URBANA, IL (LIBRARY)
UNIVERSITY OF KANSAS Kansas Geological Survey, Lawrence KS
UNIVERSITY OF MASSACHUSETTS (Heronemus), Amherst MA CE Dept
UNIVERSITY OF MICHIGAN Ann Arbor MI (Richart)
UNIVERSITY OF NEBRASKA-LINCOLN LINCOLN, NE (SPLETTSTOESSER)
UNIVERSITY OF NEW HAMPSHIRE DURHAM, NH (LAVOIE)
UNIVERSITY OF RHODE ISLAND KINGSTON, RI (PAZIS); Narragansett RI (Pell Marine Sci. Lib.)
UNIVERSITY OF TEXAS Inst. Marina Sci (Library), Port Aransas TX
UNIVERSITY OF TEXAS AT AUSTIN AUSTIN, TX (THOMPSON)
UNIVERSITY OF WASHINGTON Dept of Civil Engr (Dr. Mattock), Seattle WA; SEATTLE, WA (APPLIED PHYSICS LAB); SEATTLE, WA (OCEAN ENG RSCH LAB, GRAY); SEATTLE, WA (PACIFIC MARINE ENVIRON. LAB., HALPERN)
UNIVERSITY OF WISCONSIN Milwaukee WI (Ctr of Great Lakes Studies)
US DEPT OF COMMERCE NOAA, Marine & Earth Sciences Lib., Rockville MD
USGEOLOGICAL SURVEY Off. Marine Geology, Mailstop 915, Reston VA
VENTURA COUNTY ENVIRONMENTAL RESOURCE AGENCY VENTURA, CA (MELVIN)
VERMONT STATE ENERGY OFFICE MONTEPELIER, VT (DIRECTOR)
VIRGINIA STATE ENERGY OFF RICHMOND, VA.
AEROSPACE CORP Acquisition Group, Los Angeles CA
ARCAIR CO D Young, Lancaster OH
ATLANTIC RICHFIELD CO. DALLAS, TX (SMITH)
BECHTEL CORP SAN FRANCISCO, CA (PHELPS)
BETHLEHEM STEEL CORP, GEN.
BROWN & ROOT Houston TX (D. Ward)
CANADA Can Dive Services (English) North Vancouver; Lockheed Petrol. Srv. Ltd., New Westminster BC, Mem Univ Newfoundland (Chari), St Johns; Surveyor, Nenninger & Chenevert Inc.,
CHEVRON OIL FIELD RESEARCH CO. LA HABRA, CA (BROOKS)
COLUMBIA GULF TRANSMISSION CO. HOUSTON, TX (ENG. LIB.)
DRAVO CORP Pittsburgh PA (Giannino)
DURHAM RICHARDSON JENKINS & ASSOC. Columbia SC
NORWAY DET NORSKE VERITAS (Library), Oslo
EVALUATION ASSOC., INC KING OF PRUSSIA, PA (FEDELE)
EXXON PRODUCTION RESEARCH CO Houston TX (A. Butler Jr)
FRANCE Dr. Dutertre, Boulogne, P. Jensen, Boulogne; Roger LaCroix, Paris
GLOBAL MARINE DEVELOPMENT NEWPORT BEACH, CA (HOLLETT)
GOULD INC. Shady Side MD (Ches. Inst. Div., W. Paul)
GRUMMAN AEROSPACE CORP. Bethpage NY (Tech. Info. Ctr)
HUGHES AIRCRAFT Culver City CA (Tech. Doc. Ctr)
LOCKHEED MISSILES & SPACE CO. INC. SUNNYVALE, CA (PHILLIPS)
LOCKHEED OCEAN LABORATORY San Diego CA (F. Simpson)
MARATHON OIL CO Houston TX (C. Seay)
MCCLELLAND ENGINEERS INC Houston TX (B. McClelland)
MOBILE PIPELINE CO. DALLAS, TX MGR OF ENGR (NOACK)
NEWPORT NEWS SHIPBLDG & DRYDOCK CO. Newport News VA (Tech. Lib.)
NORWAY A. Torum, Trondheim; DET NORSKE VERITAS (Roren) Oslo; J. Creed, Ski; Norwegian Tech Univ (Brandtzaeg), Trondheim
OCEAN DATA SYSTEMS, INC. SAN DIEGO, CA (SNODGRASS)
OCEAN ENGINEERS SAUSALITO, CA (RYNECKI)
OCEAN RESOURCE ENG. INC. HOUSTON, TX (ANDERSON)

OFFSHORE DEVELOPMENT ENG. INC. BERKELEY, CA; Berkeley CA
PACIFIC MARINE TECHNOLOGY LONG BEACH, CA (WAGNER)
SWEDEN GeoTech Inst
SAFETY SERVICES, INC. A. Patton, Providence RI
SANDIA LABORATORIES Library Div., Livermore CA
SCHUPACK ASSOC SO. NORWALK, CT (SCHUPACK)
SEATECH CORP. MIAMI, FL (PERONI)
SHELL DEVELOPMENT CO. HOUSTON,, TX (TELES); Houston TX (E. Doyle)
SHELL OIL CO. HOUSTON, TX (MARSHALL); Houston TX (R. de Castongrene)
SWEDEN VBB (Library), Stockholm
TEXTRON INC BUFFALO, NY (RESEARCH CENTER LIB.)
TIDEWATER CONSTR. CO Norfolk VA (Fowler)
TRW SYSTEMS CLEVELAND, OH (ENG. LIB.); REDONDO BEACH, CA (DAI)
UNITED KINGDOM D. New, G. Maunsell & Partners, London; Shaw & Hatton (F. Hansen), London; Taylor, Woodrow Constr (014P), Southall, Middlesex; Taylor, Woodrow Constr (Stubbs), Southall, Middlesex; Univ. of Bristol (R. Morgan), Bristol
UNITED TECHNOLOGIES Windsor Locks CT (Hamilton Std Div., Library)
WESTINGHOUSE ELECTRIC CORP. Annapolis MD (Oceanic Div Lib, Bryan); Library, Pittsburgh PA
WEYERHAEUSER CO. LONGVIEW, WA (TECH CTR LIB)
WISS, JANNEY, ELSTNER, & ASSOC Northbrook, IL (J. Hanson)
WM CLAPP LABS - BATTELLE DUXBURY, MA (LIBRARY)
WOODWARD-CLYDE CONSULTANTS PLYMOUTH MEETING PA (CROSS, III)
BULLOCK La Canada
CAPT MURPHY SAN BRUNO, CA
GREG PAGE EUGENE, OR
T.W. MERMEL Washington DC